







Vaccine-Induced, High-Magnitude HIV Env-Specific Antibodies with Fc-Mediated Effector Functions Are Insufficient to Protect Infant Rhesus Macaques against Oral SHIV Infection

Alan D. Curtis II,^{a,b,c}  Pooja T. Saha,^d Maria Dennis,^e Stella J. Berendam,^e Pratamesh Ramasubramanian,^f Kaitlyn A. Cross,^d  S. Munir Alam,^e Guido Ferrari,^{e,f,g} Pamela A. Kozlowski,^h  Genevieve G. Fouda,^e Michael G. Hudgens,^d  Koen K. A. Van Rompay,ⁱ Justin Pollara,^{e,f,g} Sallie R. Permar,^j  Kristina De Paris^{a,b,c}

^aDepartment of Microbiology and Immunology, School of Medicine, University of North Carolina at Chapel Hill, Chapel Hill, North Carolina, USA

^bCenter for AIDS Research, School of Medicine, University of North Carolina at Chapel Hill, Chapel Hill, North Carolina, USA

^cChildren's Research Institute, School of Medicine, University of North Carolina at Chapel Hill, Chapel Hill, North Carolina, USA

^dDepartment of Biostatistics, Gillings School of Public Health, University of North Carolina at Chapel Hill, Chapel Hill, North Carolina, USA

^eDuke Human Vaccine Institute, Duke University Medical Center, Durham, North Carolina, USA

^fDepartment of Surgery, Duke University School of Medicine, Durham, North Carolina, USA

^gDepartment of Molecular Genetics and Microbiology, Duke University Medical Center, Durham, North Carolina, USA

^hDepartment of Microbiology, Immunology and Parasitology, Louisiana State University Health Sciences Center, New Orleans, Louisiana, USA

ⁱCalifornia National Primate Research Center, University of California at Davis, Davis, California, USA

^jDepartment of Pediatrics, Weill Cornell Medical College, New York, New York, USA

ABSTRACT Improved access to antiretroviral therapy (ART) and antenatal care has significantly reduced *in utero* and peripartum mother-to-child human immunodeficiency virus (HIV) transmission. However, as breast milk transmission of HIV still occurs at an unacceptable rate, there remains a need to develop an effective vaccine for the pediatric population. Previously, we compared different HIV vaccine strategies, intervals, and adjuvants in infant rhesus macaques to optimize the induction of HIV envelope (Env)-specific antibodies with Fc-mediated effector function. In this study, we tested the efficacy of an optimized vaccine regimen against oral simian-human immunodeficiency virus (SHIV) acquisition in infant macaques. Twelve animals were immunized with 1086.c gp120 protein adjuvanted with 3M-052 in stable emulsion and modified vaccinia Ankara (MVA) virus expressing 1086.c HIV Env. Twelve control animals were immunized with empty MVA. The vaccine prime was given within 10 days of birth, with booster doses being administered at weeks 6 and 12. The vaccine regimen induced Env-specific plasma IgG antibodies capable of antibody-dependent cellular cytotoxicity (ADCC) and phagocytosis (ADCP). Beginning at week 15, infants were exposed orally to escalating doses of heterologous SHIV-1157(QNE)Y173H once a week until infected. Despite the induction of strong Fc-mediated antibody responses, the vaccine regimen did not reduce the risk of infection or time to acquisition compared to controls. However, among vaccinated animals, ADCC postvaccination and postinfection was associated with reduced peak viremia. Thus, nonneutralizing Env-specific antibodies with Fc effector function elicited by this vaccine regimen were insufficient for protection against heterologous oral SHIV infection shortly after the final immunization but may have contributed to control of viremia.

IMPORTANCE Women of childbearing age are three times more likely to contract HIV infection than their male counterparts. Poor HIV testing rates coupled with low adherence to antiretroviral therapy (ART) result in a high risk of mother-to-infant HIV transmission, especially during the breastfeeding period. A preventative vaccine could curb pediatric HIV infections, reduce potential health sequelae, and prevent the need for lifelong ART in this population. The results of the current study imply that the HIV Env-

Editor David W. Pascual, University of Florida

Copyright © 2022 Curtis et al. This is an open-access article distributed under the terms of the [Creative Commons Attribution 4.0 International license](https://creativecommons.org/licenses/by/4.0/).

Address correspondence to Kristina De Paris, abelk@med.unc.edu.

The authors declare no conflict of interest.

Received 9 October 2021

Accepted 4 February 2022

Published 23 February 2022

specific IgG antibodies elicited by this candidate vaccine regimen, despite a high magnitude of Fc-mediated effector function but a lack of neutralizing antibodies and polyfunctional T cell responses, were insufficient to protect infant rhesus macaques against oral virus acquisition.

KEYWORDS ADCC, Fc-mediated antibody function, pediatric HIV vaccine, rhesus macaque

The successful implementation of antiretroviral therapy (ART) for women living with human immunodeficiency virus (HIV) has resulted in a drastic reduction of *in utero* and peripartum mother-to-child transmission of HIV type 1 (HIV-1) in the last 2 decades. Yet globally, between 400 and 500 infants continue to acquire HIV every day (1). The majority of these infections occur during the breastfeeding period. Limited access to ART in rural communities, HIV diagnosis late in pregnancy, gaps in linking antenatal care with postnatal mother and infant care, acute maternal infection during the breastfeeding period, and lack of ART adherence impede the prevention of HIV transmission by breast milk (2–9). Transmission of HIV can occur throughout the breastfeeding period, with a cumulative risk increase with every month of breastfeeding (10–13). However, in many resource-limited countries, breast milk remains a necessary choice for nutrition and to provide passive immunity to protect the infant against other endemic pathogens (6, 7, 14). Indeed, early weaning is associated with increased infant mortality (15–17), and the WHO recommends exclusive breastfeeding for 6 to 12 months for infants born to HIV-infected mothers (18). Infants born to mothers with known HIV-positive status are tested at birth and immediately started on ART if found to be infected, whereas infants who acquire HIV by breastfeeding often go undiagnosed until they develop clinical symptoms. Prolonged HIV replication prior to diagnosis may severely interfere with multiple aspects of normal immune and central nervous system development and impede immune reconstitution after ART initiation. Therefore, prevention strategies tailored to infants are needed to further reduce the risk of pediatric HIV infections.

In nonhuman primate (NHP) models of HIV, infection of neonatal and infant rhesus macaques (RM) with simian-human immunodeficiency virus (SHIV) can be prevented by passive administration of broadly neutralizing HIV envelope (Env)-specific antibodies (bNAbs) (19–21). The use of bNAbs as potential prevention strategy in HIV-exposed infants is supported by results from ongoing clinical trials that indicate that bNAbs (e.g., VRC01) are safe and well tolerated in human neonates (22). Clinical studies in human adults, however, demonstrated only a minimal risk reduction of HIV infection by preventative treatment with bNAbs (23, 24). Therefore, the development of an effective HIV vaccine remains a high priority for this risk group. While the induction of HIV bNAbs by vaccination remains challenging, antibodies with Fc-mediated effector function can be induced more consistently and have been associated with partial protection in multiple NHP vaccine/challenge studies (25–29) and in the human RV144 HIV vaccine trial (30). Furthermore, the protective effect of bNAbs is not due solely to their neutralization function but also depends, at least in part, on the Fc-mediated effector functions of these bNAbs (31, 32).

Utilizing the pediatric rhesus macaque model, we previously compared different HIV vaccine modalities, immunization intervals, and adjuvants to optimize the induction of HIV Env-specific IgG antibodies with Fc-mediated effector functions (33–35). Building on these results, in the current study, we tested the efficacy of an intramuscular (i.m.) vaccine consisting of a modified vaccinia Ankara (MVA) virus vector expressing transmitted/founder virus 1086.c gp120 combined with 1086.c HIV gp120 protein and 3M-052 adjuvant in stable emulsion against oral SHIV acquisition in infant macaques. Consistent with our prior findings, the vaccine induced high-magnitude Env-specific antibodies in plasma with potent antibody-dependent cellular cytotoxicity (ADCC) and antibody-dependent cellular phagocytic (ADCP) function. Nonetheless, these responses did not protect infant rhesus macaques against subsequent heterologous oral SHIV challenge.

TABLE 1 Summary of study animals

Group	Animal	Sex	Age (days) at 1st immunization	No. of challenges to achieve infection	Infecting dose	Peak viremia (copies/mL)
Mock	RM1	Female	8	17	1:100	5.1×10^7
Mock	RM2	Male	8	3	1:1,000	1.3×10^8
Mock	RM3	Male	6	13	1:1,000	2.5×10^6
Mock	RM4	Female	6	14	1:100	7.1×10^5
Mock	RM5	Male	5	7	1:1,000	7.6×10^6
Mock	RM6	Female	4	4	1:1,000	1.3×10^8
Mock	RM7	Female	10	8	1:1,000	8.9×10^6
Mock	RM8	Male	10	15	1:100	4.3×10^7
Mock	RM9	Female	7	2	1:1,000	2.1×10^7
Mock	RM10	Male	7	30	Undiluted	3.1×10^4
Mock	RM11	Male	6	2	1:1,000	1.6×10^7
Mock	RM12	Male	4	3	1:1,000	3.5×10^8
Vaccine	RM13	Female	8	3	1:1,000	5.3×10^6
Vaccine	RM14	Male	7	15	1:100	1.7×10^7
Vaccine	RM15	Male	5	24	1:10	5.1×10^5
Vaccine	RM16	Male	5	1	1:1,000	2.0×10^6
Vaccine	RM17	Male	4	4	1:1,000	1.1×10^6
Vaccine	RM18	Male	3	2	1:1,000	1.2×10^7
Vaccine	RM19	Female	8	28	1:2	9.7×10^6
Vaccine	RM20	Male	8	3	1:1,000	4.7×10^6
Vaccine	RM21	Female	7	7	1:1,000	2.1×10^6
Vaccine	RM22	Male	7	15	1:100	4.5×10^7
Vaccine	RM23	Female	6	20	1:100	5.3×10^7
Vaccine	RM24	Male	6	23	1:10	1.4×10^7

RESULTS

Study design. The current study utilized infant RM that were randomly divided into 2 groups of 12 at birth (Table 1; Fig. 1). Infant RM in the vaccine group were immunized at week 0 with 2×10^8 PFU of MVA-HIV 1086.c Env construct and 15 μ g of 1086.c gp120 protein mixed with 3M-052-SE adjuvant by the i.m. route. At weeks 6 and 12, infants in the vaccine cohort received i.m. booster immunizations with MVA-HIV Env and 1086.c gp120 protein in 3M-052-SE. In addition, to induce simian immunodeficiency virus (SIV)-specific T cell responses, infant vaccinees were primed with 5×10^{10} viral particles of ChAdOx1.tSIVconsv239 expressing conserved SIV Gag/Pol epitopes at week 0. These responses were boosted by immunizations with 2×10^8 PFU of MVA.tSIVconsv239 at weeks 6 and 12. Control infants received an empty MVA vector at weeks 0, 6, and 12 (Fig. 1). Once-weekly oral SHIV challenges were initiated at week 15, 3 weeks after the last immunization. Animals were followed for approximately 12 weeks post-SHIV infection, with infection being defined two consecutive positive viral RNA results for an animal.

Vaccine-induced 1086.c envelope-specific antibody responses. We first aimed to confirm our prior findings that the vaccine regimen induces potent HIV Env-specific antibody responses (35). Plasma 1086.c gp120-specific IgG responses were detected as early as week 3 after the first immunization in the majority of animals (Fig. 2A). Antibody levels were enhanced following the week 6 booster immunization, waned slightly thereafter, and reached peak levels after the final immunization at week 12. Geometric mean plasma HIV Env-specific IgG concentrations at week 14 (1,060,401 ng/mL; 95% confidence interval [CI], 1,470,184; 21,020) were comparable to those elicited in our prior study (1,251,467 ng/mL; 95% CI, 1,049,651; 53,481) (35). We also tested for the induction of Env-specific plasma IgA antibody in vaccinated infants (Fig. 2B). The induction of plasma Env-specific plasma IgA was delayed compared to that of plasma IgG and was of lower magnitude. Env-specific IgG and IgA were also detectable in saliva (Fig. 2C and D). The positive correlation between plasma and salivary Env-specific IgG and IgA (Fig. 2E and F) implied that antibodies in saliva likely reflected transudation

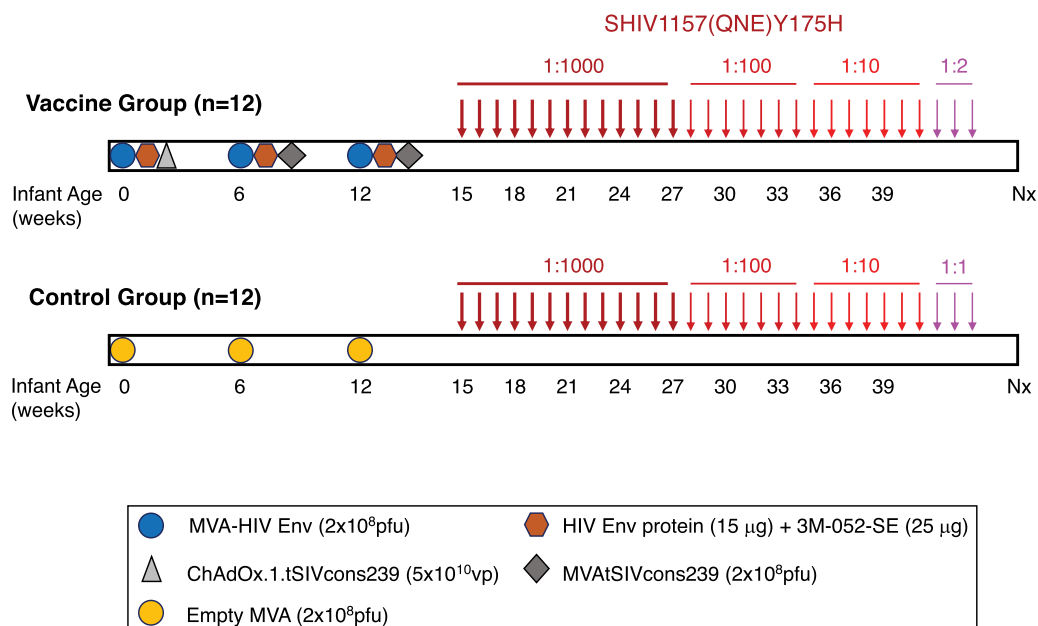


FIG 1 Experimental design. In the vaccine group, 12 neonatal rhesus macaques (Table 1) were immunized with 2×10^8 PFU of MVA-HIV Env, HIV Env protein (15 μ g) mixed with 3M-052-SE, and 5×10^{10} ChAdOx1.tSIVcons239 viral particles at week 0. Booster immunizations of 2×10^8 PFU each of MVA-HIV Env, HIV Env protein in 3M-052-SE, and MVA.tSIVcons239 were provided at weeks 6 and 12. A second cohort of 12 age-matched RM received control MVA immunizations at weeks 0, 6, and 12. Beginning at week 15, animals were challenged weekly with SHIV-1157 (QNE)Y173H viral stock diluted 1:1,000 in RPMI 1640 medium until infected. After 13 exposures, uninfected infants ($n = 11$) were exposed to a 1:100 SHIV dose for 7 weeks, a dose that was increased to 1:10 for seven more exposures in animals not infected by the 1:100 dose ($n = 4$). Two infants remained negative and became infected after challenge with 1:2 dilution of virus stock (RM19) or undiluted (1:1) virus (RM10) (Table 1). SHIV exposures are indicated by arrows with distinct shades of red based on virus dilution.

from the plasma rather than local induction at mucosal sites. The limited saliva volumes did not allow us to test for the secretory component of IgA to determine mucosal antibody production.

We next evaluated the avidity and functional potential of Env-specific plasma IgG. The avidity of plasma IgG specific for 1086.c gp120 was measured by surface plasmon resonance (SPR), and the median avidity score at week 14 was determined to be 2.4×10^7 (95% CI, 1.45×10^7 , 6.5×10^7) (Fig. 3A), an avidity similar ($P = 0.4$; Wilcoxon rank sum test) to the one in our previous study (median avidity score, 4.6×10^7 ; 95% CI, 1.2×10^7 , 9.6×10^7) (35). The avidity of plasma vaccine-elicited IgG was stronger for the clade C consensus V3 than for the V1V2 epitope of 1086.c Env (Fig. 3A). The current vaccine regimen elicited weak clade C tier 1 neutralization antibodies. In 7 of 12 vaccinated infants, the peak neutralization titers against the tier 1b virus I6644.v2.c33 were >500 at week 14, but only 5 of the 7 animals had maintained tier 1b 50% inhibitory dilution (ID_{50}) titers of >500 by week 15 (Fig. 3B).

Because a main goal of the current design was to elicit nonneutralizing antibody, we assessed the propensity of vaccine-elicited plasma antibody for FcR-mediated ADCC. ADCC responses against Env 1086.c gp120 were detectable in 75% of vaccinated infants by week 9 and in 100% by the time of initial SHIV challenge at week 15 (Fig. 3C). Similar to vaccine-induced plasma Env-specific IgG, the high ADCC endpoint titers and median granzyme B activity (Fig. 3D) in the current study were comparable to those observed in our prior study (35). To assess the ADCC activity that was independent of monocytes and could be attributed exclusively to NK cells (36), we performed area scaling (37). NK cell-mediated ADCC activity ranged from 17.8% to 45.8% (median, 33.75 [Fig. 3E]). In addition to ADCC, 1086.c Env-specific plasma antibodies were also able to mediate ADCP (Fig. 3F). Relevant to both ADCC and ADCP function, plasma IgG was capable of binding to Env 1086.c expressed on the surface of HIV-

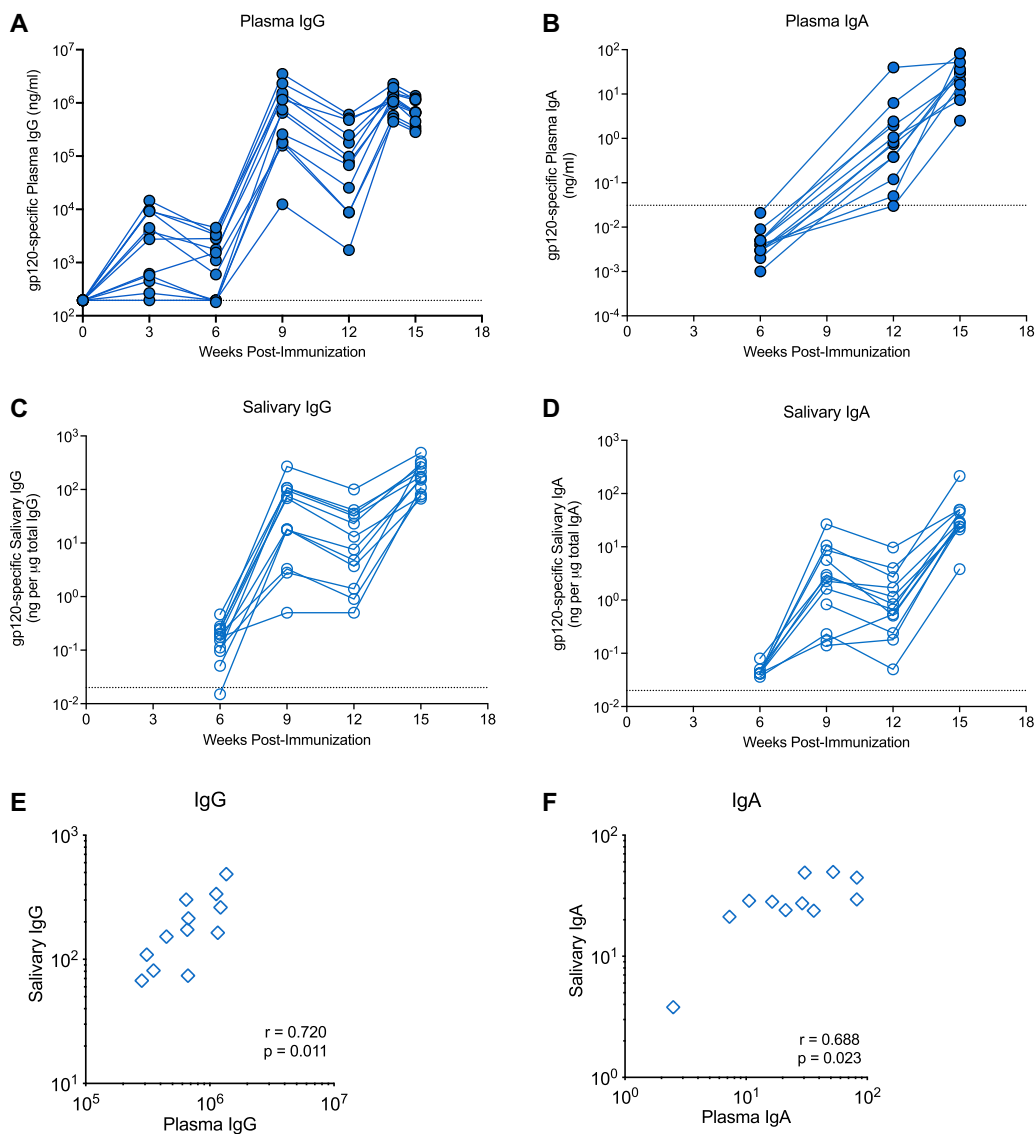


FIG 2 C.1086 Env-specific antibody responses. Plasma concentrations of 1086.c gp120-specific IgG (A) and IgA (B) were measured by ELISA and BAMA, respectively. Salivary IgG and IgA levels, measured by BAMA, are reported as specific activity in nanograms of 1086.c gp120 IgG or IgA per μ g of total IgG (C) or IgA (D). Dashed lines represent the cutoff for positivity, defined as mean antibody levels in control animals plus 3 standard deviations (SD). Panels E and F illustrate the Spearman correlation between plasma and saliva vaccine-induced IgG and IgA levels, respectively. Each symbol represents an individual animal of the 12 vaccinated animals.

infected cells (ICABA), with 11 of 12 infants having >20% binding at week 15 (range, 7.60% to 62.62%; mean, 44.70%) (Fig. 3G).

We also measured antibody responses relevant to the heterologous SHIV challenge virus, including clade C 1157ipd3N4 Env-specific IgG and 1157(QNE)Y173H Env V1V2-specific antibody responses. Although the overall magnitude of plasma binding antibodies to 1157ipd3N4 gp120 was lower than for 1086.c gp120-specific IgG, the kinetics of plasma binding antibodies to 1157ipd3N4 Env followed a pattern similar to that observed for 1086.c gp120-specific IgG. All animals developed 1157ipd3N4 gp120-specific IgG after the second immunization, with peak responses at week 14, 2 weeks after the third immunization (Fig. 4A). The median avidity score of plasma IgG against 1157id3N4 gp120 (1.9×10^6 ; 95% CI, 7.3×10^6 , 2.3×10^6) was about 1 log lower than the avidity index for the vaccine immunogen 1086.c gp120, and the avidity for the V1V2 region of 1157(QNE)Y173H was 1 log lower than the avidity for 1086.c V1V2

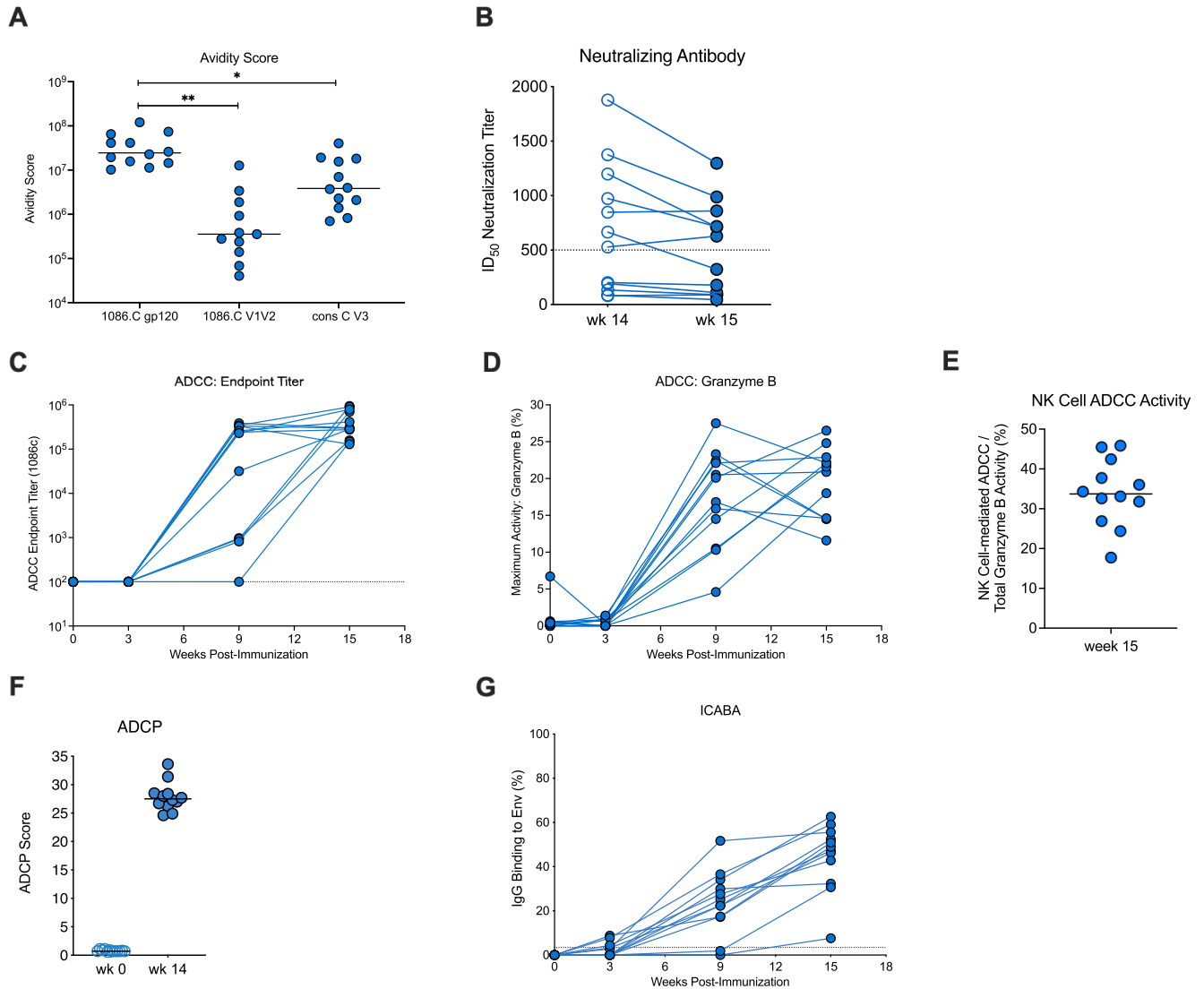


FIG 3 Prechallenge antibody function of vaccinated infant macaques. (A) Avidity score, determined by SPR, of week 15 plasma IgG specific for 1086.c gp120 or V1V2 or for the consensus clade C V3 (gp70). Each symbol represents a single animal. Note that only 11 of 12 animals were included in the testing for 1086.c V1V2 avidity due to limited plasma volumes. (B) Tier 1b clade C I6644.v2.c33 neutralization titers of vaccinated infants at week 14 and week 15. (C and D) Longitudinal data for ADCC endpoint titers and maximum granzyme B activity, with each line representing an individual animal. Dashed lines indicate the limit of detection. (E) The percentage of monocyte-independent, NK cell-mediated ADCC activity at week 15. (F) ADCP scores for vaccinated animals prior to vaccination at week 0 and week 14. (G) Plasma IgG binding to cells infected with HIV 1086.c is shown over time for individual vaccinated animals. Each time point shows data for all 12 of the vaccinated animals if not indicated otherwise.

(Fig. 3A and 4B). The vaccine regimen elicited high levels of Env-specific plasma antibodies with ADCC activity against the clade C 1157ipd3N4 gp120 (Fig. 4C), with median endpoint titers (2.89×10^5) comparable to the median titer for 1086.c (2.99×10^5 [Fig. 3B]), although ADCC 1157ipd3N4-specific IgG endpoint titers exhibited greater variability among the individual animals.

Cellular responses to vaccination. The majority of vaccinated animals developed SIV Gag-specific T cell responses by week 14 in peripheral blood (Fig. 5A). In lymph nodes, SIV Gag-specific T cell responses were detected in 9 of 12 vaccinees. (Fig. 5B). SIV Gag-specific CD4⁺ T cells appeared to produce predominantly tumor necrosis factor alpha (TNF- α) and interleukin 17 (IL-17), whereas a more mixed cytokine response was observed in CD8⁺ T cells. Polyfunctional cytokine responses were rare.

SHIV1157(QNE)Y173H challenge outcome. Starting at week 15, 3 weeks after the third immunization, animals were challenged once weekly with SHIV by the oral route. The initial virus dose consisted of 1:1,000-diluted virus stock, a dose that was purposely

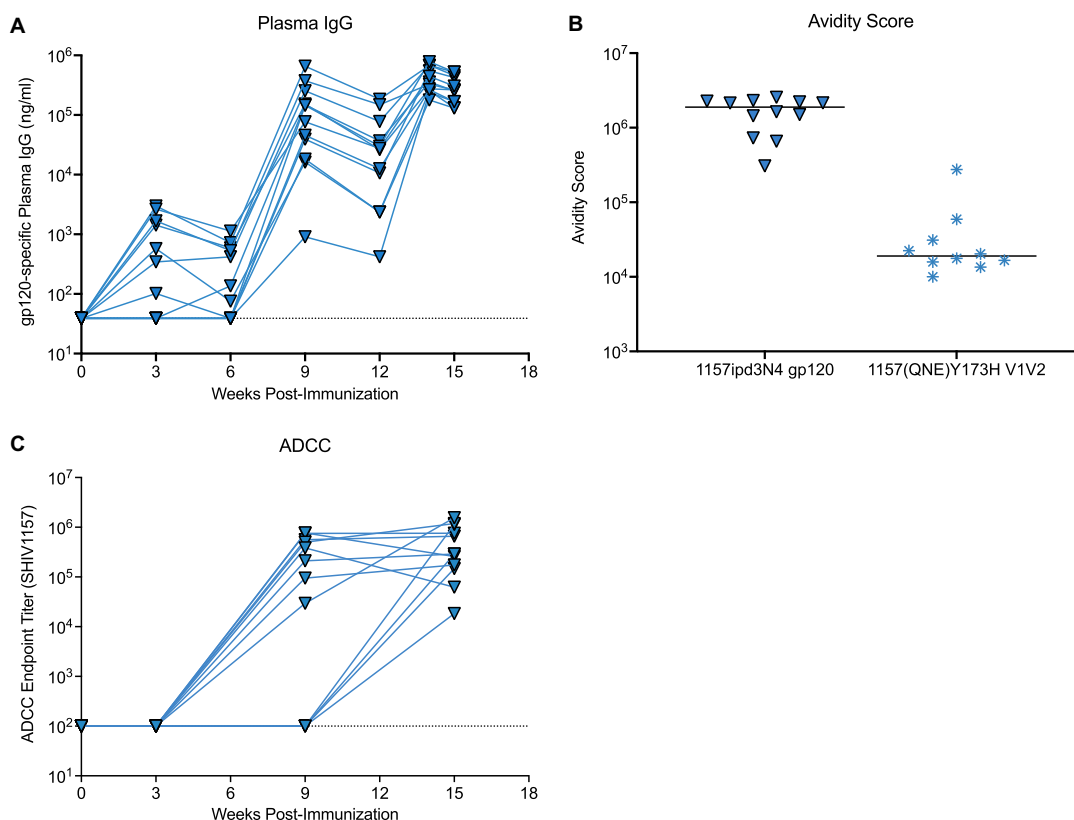


FIG 4 Vaccine-induced 1157ipd3N4 and SHIV1157(QNE)Y175H Env-specific antibody responses. (A) Plasma concentration of 1157ipd3N4 gp120-specific IgG over time in the 12 vaccinated infant rhesus macaques. (B) Avidity scores of plasma IgG specific for 1157ipd3N4 gp120 ($n = 12$) or gp70-V1V2 SHIV1157(QNE)Y375H ($n = 10$). Each symbol represents an individual animal; horizontal lines represent the medians. Note that only 10 animals could be tested for the avidity of antibodies to gp70-V1V2 SHIV1157(QNE)Y375H due to the limited plasma volumes available from infant rhesus macaques. (C) ADCC endpoint titers for plasma antibodies specific to 1157ipd3N4 gp120 in the 12 vaccinated animals.

chosen to be 10-fold higher than the dose (1:10,000) successfully used in an intrarectal (i.r.) challenge study in adult rhesus macaques (28), because of the lower risk estimate for oral versus i.r. infection determined by human HIV epidemiologic studies (38) and SHIV1157 infections in adult RM (39). Seven of 12 control vaccinated infants became infected at the 1:1,000 SHIV dose, and 4 of the remaining 5 animals became infected at 1:100. RM10 remained uninfected after 29 challenges and became infected only after oral challenge with undiluted viral stock (Fig. 6A; Table 1). The median challenge number required to become infected for control vaccinated infants was 7.5. In comparison, vaccinated animals required a median number of 11 challenges to achieve infection (Fig. 6B). Half of the vaccinated animals ($n = 6$) were infected at the 1:1,000 dose and three additional animals at the 1:100 dose. The remaining 3 animals were infected by 1:10 ($n = 2$) and 1:2 ($n = 1$) challenge virus dilutions (Fig. 6A). Although vaccinated animals required a slightly higher average number of challenges to achieve infection (11 exposures) compared to controls (7.5 exposures), there was no difference in the probability of infection at any challenge dose between the two groups ($P = 0.89$) (Fig. 6C). When we compared the probabilities of infection between control and vaccinated animals that became infected at the 1:1,000 challenge virus dose, at the 1:1,000 or 1:100 dose, or at the 1:1,000, 1:100, or 1:10 dose, we also did not detect differences in infection risks. The distributions of peak viremia also did not differ between vaccinated animals (median, 1.85×10^7 viral RNA copies/mL) and control animals (median, 7.5×10^6 viral RNA copies/mL; Wilcoxon rank sum test with exact P value of 0.24) (Fig. 6D). Similarly, there was no difference found when we compared area-under-the-curve viremia from week 0 to week 10 postinfection between the two groups ($P = 0.1978$) (Fig. 6E).

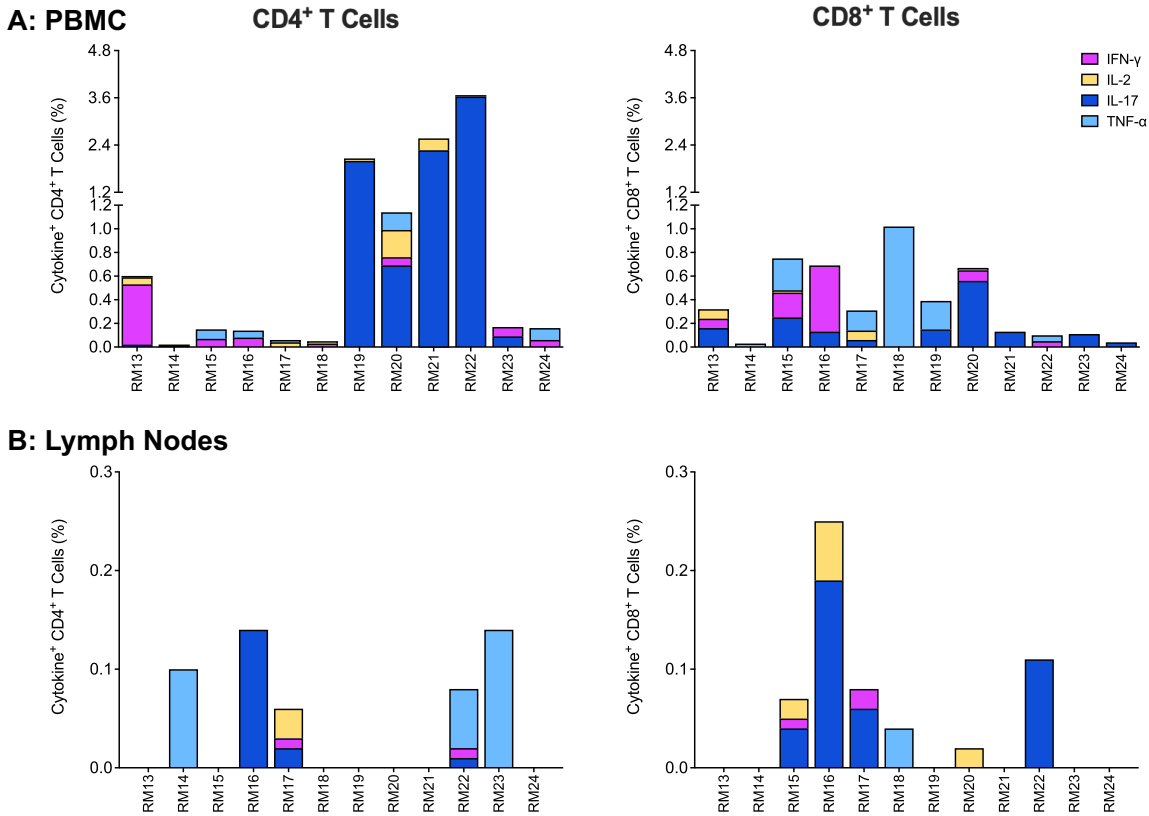


FIG 5 SIV Gag-specific T cell responses in PBMCs ($n = 12$) and peripheral lymph nodes ($n = 12$) at week 14. Each bar in panels A and B represents the sum of single cytokine responses of SIV Gag-specific CD4⁺ (left graphs) or CD8⁺ T cells (right graphs) for each vaccinated animal at week 14 in PBMCs (A) or lymph nodes (B). Cytokines measured include gamma interferon (IFN- γ), IL-2, IL-17, and TNF- α .

Immune correlates of challenge outcome. To rule out that the vaccine had caused nonspecific immune activation that could promote increased susceptibility to infection (40, 41), we tested for activation of peripheral blood CD4⁺ T cells, the main target cells for HIV. At the time of challenge initiation (week 15), we noted no difference in the frequency distributions of CCR5⁺ (CD195⁺), Ki-67⁺, CD69⁺, or CD279⁺ (PD1) CD4⁺ T cells in blood of vaccinated compared to control animals (Fig. 7). Although vaccinated animals had greater median frequencies of PD-1-positive and TNF- α -producing CD4⁺ T cells than the control group (Fig. 7), there was no correlation with this response and the number of exposures required to achieve infection (Table 2).

Despite the lack of protection against infection, we assessed whether vaccine-induced antibody responses at week 15 were associated with the number of challenges required to achieve infection (Table 2) or with peak viremia (Table 3). Although plasma IgG concentrations specific for 1086.c or 1157ipd3N4 Env were not associated with the number of exposures required to achieve infection (Table 2), there was a negative correlation between 1086.c Env-specific plasma IgG levels and peak viremia ($r = -0.657$, unadjusted $P = 0.0238$, and false-discovery-rate [FDR]-adjusted $P = 0.1426$). There was also a trend toward a negative association of salivary 1086.c Env-specific IgG ($r = -0.517$, unadjusted $P = 0.0888$, and FDR-adjusted $P = 0.3561$) and SHIV1157ipd3N4 Env-plasma IgG concentrations ($r = -0.0504$, unadjusted $P = 0.0989$, and FDR adjusted $P = 0.3561$) with peak viremia at week 15 (Table 3). We did not detect associations between plasma IgG avidity and challenge outcome. Consistent with their low titers at week 15, tier 1 neutralizing antibodies were not associated with the number of exposures required for infection or with peak viremia (Tables 2 and 3).

A more detailed assessment of Fc-mediated effector functions of Env-specific plasma IgG revealed that vaccine virus-specific ADCC activity was associated with

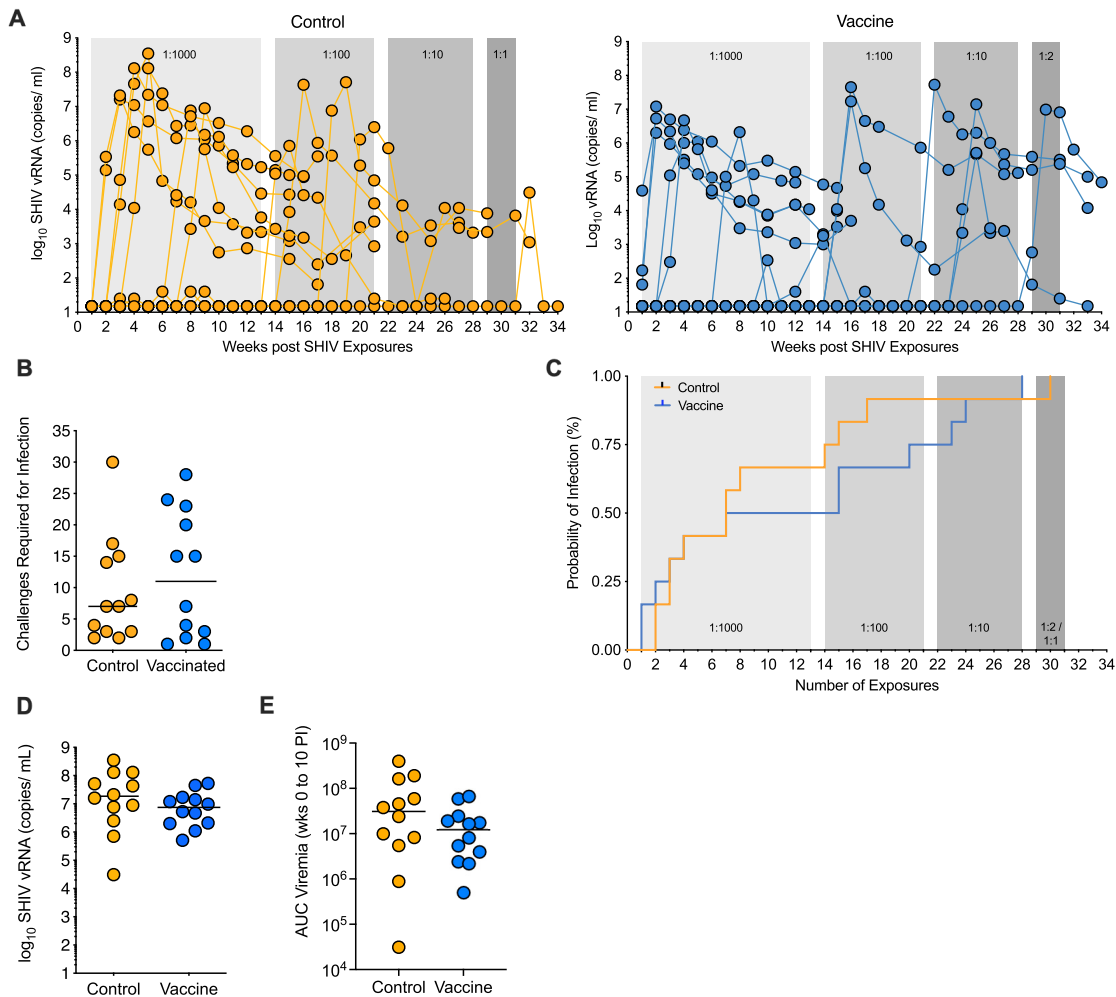


FIG 6 Challenge outcome. (A) Longitudinal plasma viral load measurements as assessed by RT-PCR from control ($n = 12$) and vaccinated ($n = 12$) cohorts of infant RM are displayed in copies per milliliter plasma. Shaded areas represent the challenge doses: light gray, 1:1000, weeks 0 to 13; medium gray, 1:100, weeks 14 to 21; dark gray, 1:10, weeks 22 to 28; darkest gray, 1:2 or undiluted. (B) The number of challenges required for infection is plotted for control ($n = 12$) and vaccinated ($n = 12$) animals. Horizontal lines represent the medians. (C) Kaplan-Meier survival curves for any dose of viral stock dilutions are shown for control and vaccinated infants. (D and E) Peak viremia (D) and area-under-the-curve (AUC) viremia from weeks 0 to 10 postinfection (PI) (E) in control ($n = 12$) and vaccinated ($n = 12$) animals. Control and vaccinated animals are indicated by orange or blue lines/symbols, respectively, with each symbol representing an individual animal; horizontal lines indicate the medians.

fewer challenges required for infection ($r = -0.761$ and unadjusted $P = 0.0054$), but this inverse correlation did not reach statistical significance after adjustment for multiple-parameter analysis (adjusted $P = 0.0984$) (Table 2). This trend was most apparent when vaccinated infant RM were stratified by median ADCC titer (2.99×10^5). The results suggested that animals with ADCC titers below the median required more SHIV exposures to become infected than animals with ADCC titers above the median (Fig. 8A). However, the probability to infection was not different between control animals, vaccinated animals with ADCC titers below the median, and vaccinated animals with ADCC titers above the median (log rank test with exact P of 0.06). Consistent with comparable median ADCC titers for 1086.c and 1157ipd3N4 Env, 1157ipd3N4 Env-specific ADCC titers trended toward a negative correlation with the number of challenges required for infection, although this trend was not substantiated after adjusting for FDR (Table 2; $r = -0.568$, unadjusted $P = 0.0580$, and FDR-adjusted $P = 0.4548$). Although ADCC activity, as assessed by maximum granzyme B production, was not correlated with the number of exposures required to achieve infection, the higher the percentage of NK cell-mediated ADCC activity, the lower was peak viremia ($r = -0.734$,

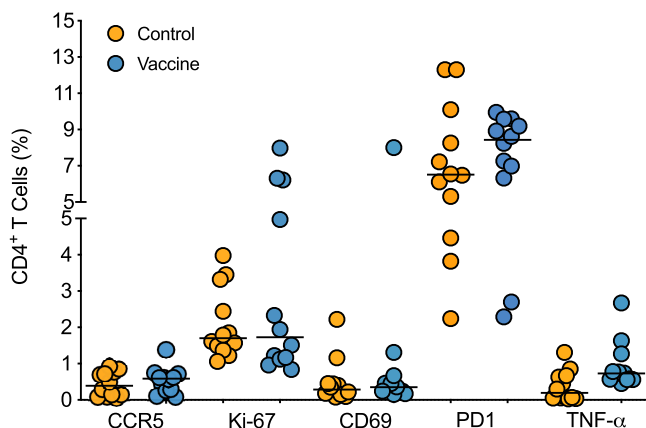


FIG 7 CD4⁺ T cell activation. PBMCs from week 15 after vaccination were gated on CD3⁺ CD4⁺ T cells and assessed for surface expression of CD195 (CCR5), CD69, and CD279 (PD1) and intracellular expression of Ki-67 and TNF- α . TNF- α -positive T cell frequencies between control ($n = 12$) and vaccinated ($n = 12$) animals were compared by Mann-Whitney test.

unadjusted $P = 0.0087$, and FDR-adjusted $P = 0.1163$) (Table 3; Fig. 8B). In contrast, ADCP function at the time of challenge initiation appeared to be positively correlated with peak viremia ($r = 0.706$, unadjusted $P = 0.0129$, and FDR-adjusted $P = 0.1163$) (Table 3).

Based on these results, and to further substantiate a potential role for Env-specific antibody responses in challenge outcome, we tested whether recall 1086.c Env-specific antibody responses at weeks 1 and 4 postinfection were associated with challenge outcome. Animals that became infected after more numbers of challenges had higher 1086.c Env-specific plasma IgG concentrations at 1 week postinfection (Table 4). Higher 1086.c Env-specific ADCC endpoint titers at 1 week postinfection, as observed at week 15 prior to challenge, were associated fewer challenges required to achieve infection (Table 4; Fig. 8C). Nonetheless, ADCC titers were negatively associated with peak viremia, and this was likely related to the finding that higher ADCC activity at week 1 postinfection was correlated with lower peak viremia (Table 4; Fig. 8D and E). However, in contrast to the ADCC activity prior to challenge, at week 4 postinfection, a higher contribution of NK cell-mediated ADCC function to ADCC activity was observed in vaccinated animals that required fewer numbers of challenges to achieve infection (Table 4; Fig. 8F). These findings emphasize the importance of the balance between magnitude and quality of immune responses in challenge outcome.

DISCUSSION

According to the UNAIDS 2021 estimates, in 2020, every day more than 400 children became infected with HIV (1). Therefore, despite increasing access to ART, vaccine development remains an urgent task to prevent new pediatric HIV infections. The current study tested the efficacy of an MVA-Env plus Env protein with 3M-052-SE adjuvant vaccine regimen combined with an ChAdOx.1.tconsSIVma239-Gag, Pol prime, MVA.tconsSIVma239-Gag, Pol boost regimen that had been optimized to maximize Env-specific antibody responses with Fc-mediated effector function (33–35, 42) in infant RM. Several previous HIV vaccine studies in NHPs had found a correlation between reduced infection or control of viral replication and vaccine-induced antibodies mediating ADCC (28, 43–45) and/or ADCP and antibody-dependent neutrophil phagocytosis (25–27). However, despite the induction of robust Env-specific antibodies with Fc-mediated effector functions, infant RM receiving the above-described vaccine regimen were not protected against oral SHIV infection. There was also no evidence of virus control, a clinically important secondary readout of vaccine efficacy pertaining to less severe disease outcomes and reduced HIV transmission risk (46).

The reasons for lack of efficacy are likely multifold. We used a challenge virus with

TABLE 2 Correlation between prechallenge immune parameters and number of challenges required for infection

Parameter	<i>n</i>	Spearman <i>r</i> value	Correlation <i>P</i> value ^c	FDR <i>p</i> -value	Figure
T cell activation ^a					
CCR5 ⁺ CD4 ⁺	24	−0.065	0.7631	0.7648	Fig. 7
Ki-67 ⁺ CD4 ⁺	24	−0.161	0.4499	0.6748	Fig. 7
CD69 ⁺ CD4 ⁺	24	0.379	0.0688	0.4131	Fig. 7
PD1 ⁺ CD4 ⁺	24	−0.064	0.7648	0.7648	Fig. 7
TNF- α ⁺ CD4 ⁺	24	−0.182	0.3913	0.6748	Fig. 7
Env-specific B cells ^b	12	−0.336	0.2845	0.6748	
Env-specific IgG ^b					
1086.c	12	−0.519	0.0864	0.4548	Fig. 2A
1157ipd3N4	12	−0.470	0.1246	0.4548	Fig. 4A
Plasma IgM ^b	11	−0.288	0.3885	0.6347	
Salivary IgG ^b	12	−0.456	0.1373	0.4548	Fig. 2C
Salivary IgA ^b	12	−0.189	0.5516	0.6818	
Avidity index ^b					
1086.c	12	−0.368	0.2365	0.5122	Fig. 3A
1157ipd3N4	12	−0.165	0.6064	0.6818	Fig. 4B
SHIV1157(QNE)Y175H	10	−0.372	0.2880	0.5190	Fig. 4B
1086.C V1V2	11	−0.119	0.7282	0.7706	Fig. 3A
gp70 ConsC V3	12	−0.428	0.1655	0.4548	Fig. 3A
Tier 1 NAb ^s ^{b,d}	12	0.023	0.9448	0.9448	
ADCC titer ^b					
1086.c	12	−0.761^e	0.0054	0.0984	Fig. 3C
1157ipd3N4	12	−0.568	0.0580	0.4548	Fig. 4C
ADCC activity ^b					
1086.c	12	−0.354	0.2561	0.5122	Fig. 3D
1157ipd3N4	12	−0.418	0.1769	0.4548	
NK cell-mediated ADCC activity ^b					
1086.c	12	−0.176	0.5829	0.6818	Fig. 3E
ADCP score ^b	12	−0.193	0.5455	0.6818	Fig. 3F
Infected cell binding ^b	12	0.242	0.4446	0.6677	Fig. 3G

^aExact *p*-value to test whether the correlation appears to be significantly different from 0.

^bFDR adjustment for multiple comparisons for the statistical analyses of cellular correlates of protection.

^cFDR adjustment for multiple comparisons for the statistical analyses of antibody correlates of protection.

^dI₅₀ neutralizing antibody titers at week 15.

^eBold values indicate Spearman rank test with *r* > 0.6 and unadjusted *p* < 0.05.

an Env that was heterologous to the vaccine immunogen and started challenges shortly (3 weeks) after the last vaccine immunization to closely mimic consistent, real-world exposure of infants breastfed by HIV-infected women. It is possible that some residual activation in response to immunization was still lingering. We (40, 41) and others (47–50) had previously reported that T cell activation can contribute to an enhanced risk of infection with HIV, SIV, or SHIV. Although we observed higher frequencies of TNF- α -positive peripheral blood CD4⁺ T cells at the time of the first challenge in vaccinated compared to control animals, T cell activation was not correlated with the number of SHIV challenges required for infection.

In our studies leading up to the current vaccine study (33–35, 41, 42), we had focused on the optimization of Fc-mediated Env-specific IgG responses. Our vaccine regimen was not designed to induce tier 2 neutralizing antibodies that are thought to be essential in the protection against SHIV infection in RM (51). We had further reasoned that the inclusion of chimpanzee adenovirus (ChAd)- and MVA-vectored vaccines expressing SIV Gag and Pol would induce antiviral T cell responses capable of controlling virus replication at the entry site. However, SIV Gag-specific T cell responses elicited by the ChAd- and MVA-vectored vaccines were of relatively low magnitude, and neither peripheral blood mononuclear cell (PBMC) nor lymph node CD4⁺ and CD8⁺ T cell responses at week 14 correlated with the number of challenges to achieve infection or with peak viremia.

TABLE 3 Correlation between vaccine-induced antibody responses at week 15 and peak viremia

Parameter	<i>n</i>	Spearman <i>r</i> value	Correlation <i>p</i> value ^b	FDR ^a <i>p</i> -value	Figure
Env-specific IgG ^a					
1086.c	12	−0.657^c	0.0238	0.1426	Fig. 2A
1157ipd3N4	12	−0.504	0.0989	0.3561	Fig. 4A
Plasma IgM ^a	11	−0.282	0.4023	0.7761	
Salivary IgG ^a	12	−0.517	0.0888	0.3561	Fig. 2C
Salivary IgA ^a	12	−0.112	0.7329	0.7761	
Avidity index ^a					
1086.c	12	−0.168	0.6039	0.7761	Fig. 3A
1157ipd3N4	12	0.196	0.5431	0.7761	Fig. 4B
SHIV1157(QNE)Y175H	10	−0.152	0.6821	0.7761	Fig. 4B
1086.C V1V2	11	−0.064	0.8603	0.8603	Fig. 3A
gp70 ConsC V3	12	−0.245	0.4434	0.7761	Fig. 3A
Tier 1 NAb ^s ^d	12	−0.112	0.7277	0.7761	
ADCC titer ^a					
1086.c	12	−0.238	0.4572	0.7761	Fig. 3C
1157ipd3N4	12	−0.196	0.5431	0.7761	Fig. 4C
ADCC activity ^a					
1086.c	12	−0.375	0.2280	0.6839	Fig. 3D
1157ipd3N4	12	−0.217	0.4990	0.7761	
NK cell-mediated ADCC ^a					
1086.c	12	−0.734	0.0087	0.1163	Fig. 8B
ADCP score ^a	12	0.706	0.0129	0.1163	Fig. 3F
Infected cell binding ^a	12	−0.147	0.6509	0.7761	Fig. 3G

^aFDR adjustment for multiple comparisons for the sets of tests specified in Materials and Methods for the statistical analysis of antibody correlates of protection.

^bExact *p*-value to test whether the correlation appears to be significantly different from 0.

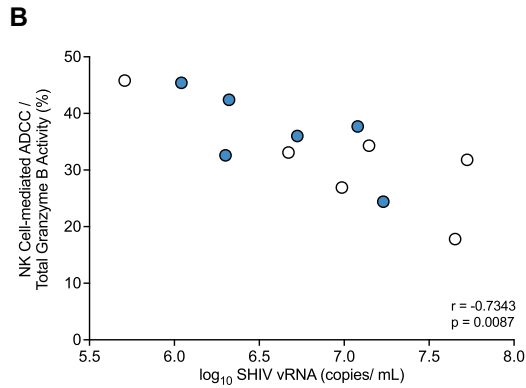
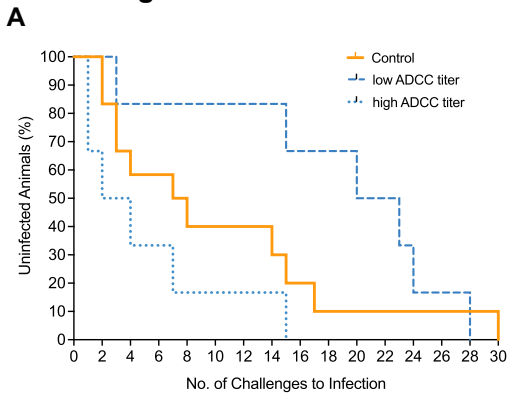
^cBold values indicate Spearman rank correlations with $r > -0.6$ and unadjusted $p < 0.05$.

^dI_{D50} neutralizing antibody titers at week 15.

Our challenge outcome results are consistent with those of other infant and adult NHP studies that failed to demonstrate efficacy against SIV or SHIV infection by antibodies with Fc-mediated effector function only (51–53), and human HIV vaccine trials following and building on the results of the RV144 trial did not observe a reduced HIV infection risk. In the RV144 trial, protective ADCC function was primarily associated with V1V2- and C1-specific antibodies (54, 55). Our vaccine regimen, however, appears to be biased toward the induction of V3 over V1V2-specific and C5- versus C1-specific epitopes (35). Furthermore, plasma IgG responses specific to the V1V2 region of the vaccine 1086.c Env and of the challenge virus SHIV1157(QNE)Y173H were of lower avidity than the relevant gp120-specific IgG. Limited plasma volumes prevented us from assessing ADCC and ADCP activity of epitope-specific antibodies in addition to gp120-specific antibodies in the current study. In future studies, more targeted, epitope-specific analyses—including impact of glycosylation and epitope conformation—may prove beneficial in the interpretation of vaccine outcomes (55, 56).

It is also important to note that the detailed analysis of RV144 results found that trial participants with medium levels of ADCC activity had reduced infection risk compared to that of participants with low levels of ADCC activity, while there was no such difference found when comparing those with high and low vaccine-induced ADCC responses (see supplement to reference 54). In the current study, 1086.c-specific plasma antibodies with ADCC activity could be detected at a median endpoint titer of 1:10⁵ at the time of challenge initiation. Paradoxically, although individual animals with high ADCC titers (above the group median) were as likely to acquire infection as their control counterparts, 1086.c ADCC titers below the median appeared to be associated with more challenges to achieve infection, although this difference did not reach statistical significance. One potential explanation for this observation is an *in vivo* prozone, a phenomenon when high antibody in the presence of limiting antigen results in smaller

Pre-Challenge



Post-Challenge

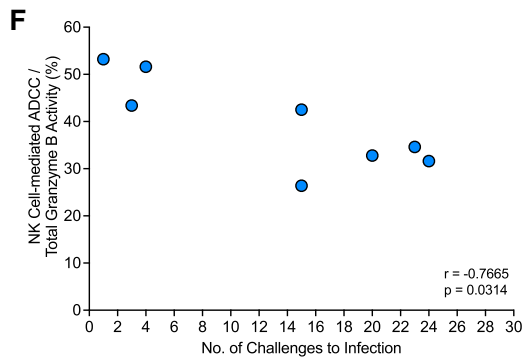
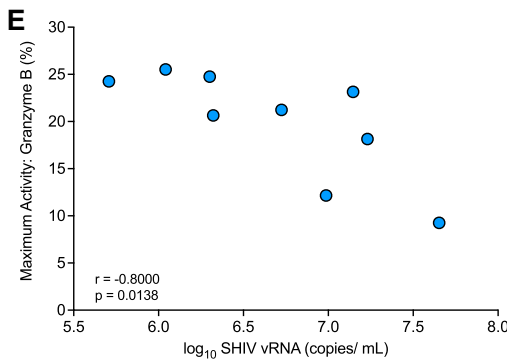
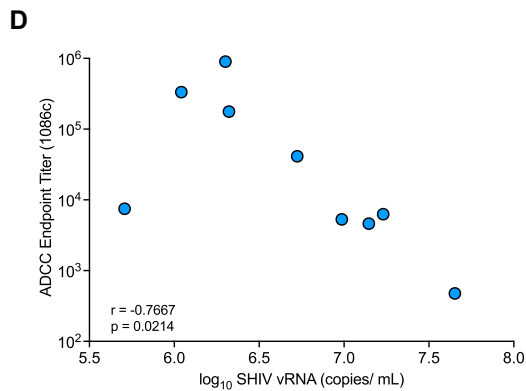
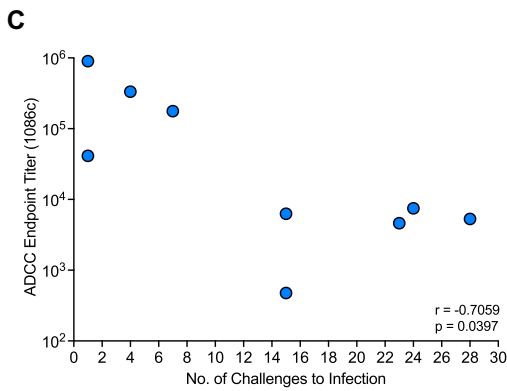


FIG 8 Correlation between 1086.c Env-specific antibody responses and challenge outcome. (A) Kaplan-Meier plot to demonstrate the relationship between ADCC endpoint titers and number of challenges required for infection when vaccinated animals are categorized as having a low ($n = 6$) or high ($n = 6$) ADCC titer based on the median ADCC endpoint titer of 10^5 in comparison to control animals ($n = 12$). Mantel-Cox log rank test was applied to determine differences in the risk of infection between groups. (B) Graph of the Spearman rank correlation between ADCC endpoint titers and number of challenges required for infection of each vaccinated animal ($n = 12$). Animals with ADCC titers below or above the median ADCC endpoint titer are indicated by empty or filled blue circles, respectively. Panels C to F illustrate correlation between Env-specific antibody responses postinfection and challenge outcome. Note that limited plasma volumes did not allow us to assess postinfection antibody responses in all 12 vaccinated animals. Panels C and D show the negative correlation of endpoint 1086.c ADCC titers at week 1 postinfection with the number of challenges required for infection (C) and peak viremia (D) for 9 vaccinated animals. Panel E illustrates that higher ADCC activity at week 1 postinfection was associated with reduced peak viremia ($n = 9$). (F) In animals that required fewer challenge exposures to infection, the percentage of NK cell-mediated ADCC activity at week 4 postinfection was higher than in animals that required a greater number of exposures to infection ($n = 8$).

immune complexes that cluster fewer Fc domain receptors on the surface of target cells and limit killing activity (57, 58). A prozone effect was also described in an early HIV infection study (59) in which plasma IgG concentrations above $10 \mu\text{g/mL}$ inhibited NK cell lysis. The importance of NK cells in ADCC-mediated protection by Env-specific

TABLE 4 Correlation between 1086.c Env-specific recall antibody responses and challenge outcome

Challenge outcome/parameter	<i>n</i>	Spearman <i>r</i> value	Correlation <i>p</i> value ^a	FDR ^b <i>p</i> -value	Figure
No. of exposures to infection					
Env-specific IgG					
Wk 1 postinfection	10	-0.677^c	0.0366	0.1588	Fig. S1 in the supplemental material Fig. S1
Wk 4 postinfection	9	-0.544	0.1356	0.4484	
ADCC titer					
Wk 1 postinfection	9	-0.706	0.0397	0.1588	Fig. 8C
Wk 4 postinfection	8	-0.180	0.6984	0.6984	
ADCC activity					
Wk 1 postinfection	9	-0.412	0.2702	0.4484	
Wk 4 postinfection	8	0.270	0.5579	0.6199	
NK cell-mediated ADCC					
Wk 1 postinfection	9	-0.395	0.2912	0.4484	Fig. 8F
Wk 4 postinfection	8	-0.766	0.0314	0.1588	
ADCP score					
Wk 1 postinfection	9	-0.378	0.3129	0.4484	
Wk 4 postinfection	8	-0.515	0.1982	0.4484	
Peak viremia					
Env-specific IgG					
Wk 1 postinfection	10	-0.418	0.2325	0.4484	Fig. S1
Wk 4 postinfection	9	-0.433	0.2499	0.4484	
ADCC titer					
Wk 1 postinfection	9	-0.767	0.0214	0.1588	Fig. 8D
Wk 4 postinfection	8	-0.571	0.2000	0.4484	
ADCC activity					
Wk 1 postinfection	9	-0.800	0.0138	0.1588	Fig. 8E
Wk 4 postinfection	8	-0.321	0.4976	0.5892	
NK cell-mediated ADCC					
Wk 1 postinfection	9	-0.367	0.3362	0.4484	
Wk 4 postinfection	8	-0.405	0.3268	0.4484	
ADCP score					
Wk 1 postinfection	9	-0.200	0.6134	0.6457	
Wk 4 postinfection	8	0.286	0.5008	0.5892	

^aExact *p*-value to test whether the correlation appears to be significantly different from 0.

^bFDR adjustment for multiple comparisons for the sets of tests specified in Materials and Methods for the statistical analysis of antibody correlates of protection.

^cBold values indicate Spearman rank correlations with $r > -0.6$ and unadjusted $p < 0.05$.

antibodies was underlined by our findings that NK cell-mediated ADCC activity prior to challenge at week 15 was associated with reduced peak viremia. These data, and data from passive immunization of mice (60), suggest that there may be an optimal level, with lower and upper limits, at which nonneutralizing antibodies are most effective. However, what these levels are in the context of different exposures and how they potentially impact challenge outcome are not yet known.

Similarly, it is difficult to discern from the current literature whether there is an optimal ADCP score. Despite several studies suggesting a correlation between ADCP function and reduced HIV risk in human adults (61, 62) or SHIV infection in adult RM (25), ADCP activity elicited by the vaccine tested in the current study was not correlated with protection against oral SHIV1157(QNE)Y375H infection in infant RM. While the simple comparison of various antibody functions across different vaccine regimens, age groups, and challenge regimens is likely flawed, and different assay conditions may further impact data, the results of our study imply that the magnitude of ADCC or ADCP activity alone is not a reliable predictor of vaccine efficacy. More research is needed to assess the impact of antibody subtype, effector cell and specific Fc receptors mediating the specific functions on vaccine efficacy in preclinical NHP studies (63), and how these findings translate to humans (64). Such findings would likely result in improved *in vitro* assays to measure antibody function and thereby enhance the predictive value of these assays for vaccine efficacy assessment. Highly relevant for pediatric studies, age-dependent differences in immune function of effector cells are not considered. There are numerous studies documenting that NK cells and monocytes exhibit reduced functional capacity, including ADCC (65) and phagocytosis, in infants

compared to adults (see reviews in references 66 to 70). Few studies have examined the expression of FcR γ I, FcR γ II, and FcR γ III on infant NK cells, monocytes, and neutrophils (71, 72). Therefore, in future studies, we will expand the analysis of vaccine-induced B and T cell responses and also determine whether and how pediatric HIV vaccine regimens impact innate immune cells and their functions.

In summary, while the prechallenge immunogenicity data demonstrated high magnitude effector antibody functions previously tied to some HIV vaccine efficacy, our results imply that Env-specific ADCC and ADCP responses induced by this candidate vaccine regimen were not sufficient to prevent infection with oral tier 2 SHIV1157 (QNE)Y375H in infant RM. Therefore, future studies of interventions to protect infants against HIV acquisition through breastfeeding should focus on improving the breadth of the antibody response, namely, the induction of bNAbs or passive administration of combinations of long-acting HIV bNAbs, as well as overcoming the relative paucity of cell-mediated immunity induced by current vaccine platforms in early life.

MATERIALS AND METHODS

Animals and sample collection. Twenty-four infant rhesus macaques (RM) were nursery reared and housed in pairs at the California National Primate Research Center (Davis, CA). All animal procedures were approved by the UC Davis Institutional Animal Care and Use Committee. The study strictly adhered to the guidelines outlined in the *Guide for the Care and Use of Laboratory Animals* (73) by the National Resource Council. Peripheral blood was collected by venipuncture into EDTA-treated vacutainers and processed as described previously (74). Peripheral lymph node biopsy specimens were collected at week 14 prior to initiation of oral challenges at week 15 as described previously (33). All experimental manipulations were performed under ketamine anesthesia (10 mg/kg of body weight) administered by the intramuscular (i.m.) route.

Vaccines. The infants in the present study were randomly divided into 2 groups of 12 (Table 1; Fig. 1). At week 0, infant RM assigned to the vaccine arm were primed i.m. with 2×10^8 PFU of MVA-HIV 1086.c Env construct (in a volume of 0.25 mL divided over the left and right biceps) (35) and 15 μ g of 1086 Δ 7 gp120 K160N protein mixed with 3M-052 adjuvant in stable emulsion (3M-052-SE) (34, 35) at a total dose volume of 0.5 mL, divided over the left and right quadriceps. The HIV Env 1086.c gp120-expressing MVA construct was produced as detailed elsewhere (75). In addition, infant vaccinees received 5×10^{10} viral particles of chimpanzee adenovirus (ChAdOx1.tSIVconsV239)-SIV Gag/Pol (0.25 mL i.m. divided over the left and right gluteus) at week 0. Infants in the vaccine cohort received two successive i.m. booster immunizations with 1086.c gp120 protein in 3M-052-SE and MVA-HIV Env (both were the same dose as the priming immunization) and 2×10^8 PFU of MVA.tSIVconsV239 (Gag/Pol-expressing vector) in 0.25 mL, divided over the left and right biceps) at weeks 6 and 12 (35). The ChAdOx1.tSIVconsV239 and MVA.tSIVconsV239 vectors were kindly provided by Tomáš Hanke (Oxford University, Oxford, UK) to promote the induction of SIV-specific T cell responses. Control infants received an empty MVA vector at weeks 0, 6, and 12 (Fig. 1).

SHIV-1157(QNE)Y173H challenge of vaccinated and control macaques. At week 15, 3 weeks after the last immunization, infant macaques were orally exposed once weekly to tier 2 SHIV-1157(QNE)Y173H, a derivative of the CCR5-tropic clade C SHIV-1157ipd3N4 (28), which was kindly provided by Sampa Santra (Harvard University, Boston, MA). The virus stock corresponded to 3.7×10^9 copies/mL and had a 50% tissue culture infective dose (TCID₅₀) of 4.88×10^8 mL in TZM-bl cells (28, 76). SHIV-1157(QNE)Y173H (referred to here as SHIV) was selected for its high sequence homology to the 1086.c V1V2 region (28). Virus was administered as a 1:1,000 dilution of virus stock in 1 mL of sucrose-containing RPMI 1640 medium in a needleless syringe (77). Infants were considered to be systemically infected following two consecutive PCR-positive values (see below). After 13 challenges of 1:1,000, uninfected infants ($n = 11$) received an increased dose of 1:100. Following 7 challenges with 1:100-diluted virus, the viral challenge was increased to a 1:10 dilution in the remaining uninfected animals ($n = 4$). Two infants (RM19 and RM10) remained negative and became infected after challenge with a 1:2 dilution of virus stock or undiluted virus, respectively (Table 1). Approximately 12 weeks post-SHIV infection, animals were euthanized.

SHIV RNA quantification. Weekly quantitative analysis of SHIV RNA in plasma began on week 16 as previously described (74). Briefly, RNA was manually extracted from limited plasma volumes and assayed by reverse transcription-PCR (RT-PCR) with a limit of detection of 15 copies/mL. Data are reported as the number of SHIV RNA copy equivalents per milliliter of EDTA plasma.

Measurement of plasma HIV Env-specific IgG by ELISA. HIV Env-specific antibody concentrations in plasma were determined by enzyme-linked immunosorbent assay (ELISA) (33). Microtiter plates were coated with 1086 Δ 7 gp120K160N (3 μ g/mL) overnight at 4°C and blocked with phosphate-buffered saline (PBS) plus 4% whey, 15% normal goat serum, and 0.5% Tween 20. Serially diluted plasma was added to the plate following extensive washing. IgG antibodies were detected with peroxidase-labeled anti-monkey IgG (Southern Biotech), followed by tetramethylbenzidine (TMB; KPL) and stop solution. Absorbance was read at 450 nm immediately after addition of the stop solution. The rhesusized CD4 binding site monoclonal antibody B12R1 was used as a standard (78). The concentration of HIV Env-specific IgG was calculated using a five-parameter fit curve relative to the standard using SoftMax Pro 6.3

software (Molecular Devices). To account for nonspecific binding, the positivity cutoff was selected as the concentration corresponding to 3 times the optical density (OD) of blank wells.

Measurement of Env-specific antibodies by binding antibody multiplex assay (BAMA). Salivary IgG and IgA and plasma IgA antibodies to gp120 were measured using a customized multiplex assay with 1086.cΔ7 gp120-conjugated fluorescent magnetic beads as previously described (33). Prior to performing IgA assays, specimens were depleted of IgG using protein G Sepharose (GE Healthcare) as described previously (79). Concentrations of gp120-specific antibodies in saliva were normalized relative to the total IgA or IgG concentrations, which were measured by ELISA. Results for saliva are presented as specific activity (nanograms of anti-gp120 IgA or IgG antibody per microgram of total IgA or IgG, respectively).

Antibody avidity. The avidity of IgG antibodies to 1086.cΔ7 gp120, 1086.C V1V2, gp70 consensus C V3 (33), 1157ipd3N4 gp120, and 1157(QNE)Y173H V1V2 was determined using purified total plasma IgG and surface plasmon resonance (SPR) using a Biacore 4000 instrument as described previously (33). The relative avidity score equals the binding response divided by the dissociation rate constant.

ADCC. Antibody-dependent cellular cytotoxicity (ADCC) activity was measured as previously reported (42). Briefly, CCR5⁺ CEM.NK^R T cells (AIDS Reagent Program) were coated with 1086.c or SHIV-1157ipd3N4 gp120 protein. ADCC activity was determined by the GranToxiLux (GTL) assay as described previously (33, 42, 80). Fourfold serial plasma dilutions beginning at 1:100 were incubated with target cells and human PBMCs from a cryopreserved leukapheresis sample of an HIV-seronegative donor with the 158F/V genotype for FcγRIIIa after thawing and overnight rest (80–82). ADCC function is reported as endpoint titers determined by interpolation of plasma dilutions that intercepted the positive cutoff and as the maximum proportion of target cells positive for active granzyme B (maximum activity). To determine the contribution of NK cells to ADCC activity, we applied area scaling analysis as described previously (37).

Infected cell antibody binding assay (ICABA). Plasma antibody binding to HIV-1 Env expressed on surfaces of infected cells was measured using an infected cell binding assay as previously described (28, 83). Briefly, CEM.NK^R cells were mock infected or infected with a replication-competent infectious molecular clone virus encoding 1086.c Env (84) for 48 to 72 h. Cells were then cultured in the presence of diluted plasma samples from study infants. Cells were subsequently stained with a viability marker, anti-CD4 antibody (clone OKT4; eBioscience), fixed, and permeabilized prior to staining with a fluorescein isothiocyanate (FITC)-conjugated goat anti-rhesus IgG (H+L) polyclonal antibody (Southern Biotech). Data represent the frequency of cells positive for IgG binding to Env for postvaccination samples compared to the prevaccination sample. Values were normalized by subtraction of the frequency of positive cells observed for cells stained with secondary antibody alone and mock-infected cells.

ADCP. Antibody-dependent cellular phagocytosis (ADCP) assay was performed as previously described (85, 86). HIV Env 1086.c K160N gp120 protein was produced in-house by transfection of 293T cells. For ADCP, the HIV Env 1086.c K160N gp120 protein was conjugated to biotin using a fast type A biotin conjugation kit (Abcam) and then captured on avidin-labeled fluorescent beads (NeutrAvidin; Invitrogen). To form immune complexes with Env-expressing beads, plasma (1:50 dilution), positive antibody controls (HIVIG, RIVIG, and VRC01), or irrelevant antibody control (influenza virus-specific monoclonal antibody CH65) was incubated with antigen-conjugated beads at 37°C for 2 h. All monoclonal antibody controls were used at a concentration of 25 μg/mL. Immune complexes were then subjected to spinoculation at 1,200 × *g* in the presence of a human-derived monocyte line, THP-1 (ATCC TIB-201), for 1 h at 4°C. Following spinoculation, bead-conjugated antigens and cells were incubated at 37°C to allow for phagocytosis to occur. After 1 h of incubation, THP-1 cells were fixed with 2% paraformaldehyde (Sigma) and fluorescence of the cells was assessed by flow cytometry (BD; Fortessa). A “no antibody” control consisting of PBS supplemented with 0.1% bovine serum albumin (1 × PBS plus 0.1% BSA) was used to determine the background phagocytosis activity. Phagocytosis scores were calculated by multiplying the mean fluorescence intensity (MFI) and frequency of bead-positive cells and dividing by the MFI and frequency of bead-positive cells in the PBS/BSA control. All plasma samples were tested in two independent assays, and the average phagocytosis scores from these 2 independent assays was reported.

Neutralizing antibody characterization. Neutralizing antibodies were tested as previously reported (87). Briefly, serum was heat inactivated for 1 h at 56°C, diluted in cell culture medium, and preincubated with HIV-1 pseudotyped virus (88) for 1 h. Following preincubation, TZM-bl cells were added and incubated for 48 h. Cells were subsequently lysed and luciferase activity was determined using a luminometer and BriteLite Plus reagent (PerkinElmer). Neutralization titers were defined as the serum dilution which reduced relative light units by 50% relative to control wells after background subtraction.

Flow cytometric analysis. (i) T cell activation. PBMCs were isolated from blood as previously described (74). A total of 10⁶ PBMCs were stained with surface antibodies listed in Table 5 at room temperature for 20 min in the dark. Cells were treated with Cytofix/Cytoperm (BD Biosciences) per the manufacturer's protocol and subsequently stained with intracellular marker antibodies (Table 5) in the same manner. Stained cells were fixed with 1% paraformaldehyde (Electron Microscopy Services). A total of 300,000 events were collected using a BD LSRFortessa and analyzed using FlowJo v10.6.1.

(ii) SIV Gag-specific T cell responses. SIV Gag-specific T cell responses were determined as described previously (89). Briefly, 2 × 10⁶ cells were cultured in RPMI 1640 medium supplemented with glutamine, 10% heat-inactivated fetal bovine serum (FBS), and penicillin/streptomycin and stimulated with a vehicle (dimethyl sulfoxide [DMSO]), 0.5 × cell stimulation cocktail (eBioscience), or 5 μg of SIV p27Gag peptide pool (NIH AIDS Reagent Program) for 6 h, with 1 × brefeldin A present after the first hour. Cells were stained with antibodies (Table 5) and analyzed as described above.

Statistical analyses. Statistical tests were performed using R version 3.6.2.

(i) Probability of infection. Kaplan-Meier curves and log rank tests with exact *P* values were used to assess differences between the two groups in the probability of infection at any challenge dose. We

TABLE 5 FACS reagent information^a

Panel/marker	Type	Fluorochrome	Clone	Vendor
Activation				
Viability dye	Surface	Aqua	NA	Invitrogen
CD3	Surface	BV421	SP34-2	BD Biosciences
CD4	Surface	PerCP-Cy5.5	L200	BD Biosciences
CD8	Surface	Alexa Fluor 700	RPA-T8	BD Biosciences
CD14	Surface	BV786	M5E2	BD Biosciences
CD16	Surface	PE-CF594	3G8	BD Biosciences
CD20	Surface	APC-H7	2H7	BD Biosciences
CD69	Surface	PE-Cy7	FN50	BD Biosciences
CD195	Surface	PE	3A9	BD Biosciences
HLA-DR	Surface	BV711	G46-6	BD Biosciences
PD-1	Surface	APC	eBioJ105	eBioscience
Ki-67	Intracellular	FITC	B56	BD Biosciences
TNF- α	Intracellular	BV650	Mab11	BD Biosciences
Antigen-specific T cells				
Viability dye	Surface	Aqua	NA	Invitrogen
CD3	Surface	APC-Cy7	SP34-2	BD Biosciences
CD4	Surface	PE-CF594	L200	BD Biosciences
CD8	Surface	BV786	RPA-T8	BD Biosciences
CD45RA	Surface	V450	5H9	BD Biosciences
CCR7	Surface	PE-Cy7	3D12	BD Biosciences
IL-2	Intracellular	PerCP-Cy5.5	MQ1-17H12	BD Biosciences
IL-17	Intracellular	PE	eBio64CAP17	BD Biosciences
IFN- γ	Intracellular	Alexa Fluor 700	B27	BD Biosciences
TNF- α	Intracellular	APC	Mab11	BD Biosciences

^aAbbreviations: FACS, fluorescence-activated cell sorting; NA, not applicable; PerCP, peridinin chlorophyll protein; PE, phycoerythrin; APC, allophycocyanin.

presented curves and tested for differences in the probability of infection at any dose. One animal missed seven weekly challenges before resuming challenges on the 1:100 dose and becoming infected on its first 1:100 dose challenge. Thus, the animal was treated as censored at its seventh challenge, (a 1:1,000 dose). We estimated the per-challenge probability of infection at each dose administered (1:1,000, 1:100, 1:10, 1:2, and 1:1) as the number of animals infected by a challenge at the dose/total number of challenges (across and within all animals) administered up to and including the week of infection at the dose. For each per-challenge probability of infection, we constructed an approximate 95% confidence interval (Wilson score interval without continuity correction) by assuming that all challenges across and within animals are independent.

(ii) Antibody correlates of protection. We assessed the association of Env-specific plasma IgG, salivary IgG, salivary IgA, antibody avidity, neutralizing antibodies, ADCC, infected cell binding, and ADCP at week 15 with the number of challenges required to achieve SHIV infection in vaccinated animals only (Table 2). The same antibody response parameters were assessed in association with peak viremia (Table 3). Spearman's rank correlation coefficients were estimated to assess these associations. All correlations were tested with exact *P* values to assess whether any were significantly different from 0. To adjust for multiple comparisons, the Benjamini-Hochberg (BH) procedure was used to control the false-discovery rate (FDR). An adjustment to control the FDR at a value of 0.05 was performed for these endpoints for a total 18 parameters per infection outcome.

Furthermore, to determine the impact of memory Env-specific plasma IgG, ADCP, and ADCC responses at week 1 and week 4 postinfection on challenge outcome, we tested whether these vaccine-induced recall antibody responses were associated with the number of challenges required to achieve SHIV infection or with peak viremia. All correlations were tested with exact *P* values to assess whether any were significantly different from 0, and the BH procedure was used to adjust for multiple comparisons. An adjustment to control the FDR at a value of 0.05 was performed for these endpoints for a total 20 parameters (Table 4).

(iii) Cellular correlates of protection. Wilcoxon rank sum tests with exact *P* values were used to compare the CCR5⁺ (CD195⁺), Ki-67⁺, CD69⁺, and CD279⁺ (PD1) CD4⁺ T cells at week 15 between vaccinated and control animals. An adjustment to control the FDR at an α value of 0.05 was performed for these 5 endpoints using the BH procedure.

Spearman's rank correlation coefficients were estimated for the cohort as a whole as well as for vaccinated animals only. All correlations were tested with exact *P* values to assess whether any were significantly different from 0. The entire cohort was used to assess whether there was an association between CD4⁺ T cell activation parameters at week 15 and the number of challenges required for SHIV infection. Vaccinated animals were used to assess whether there appeared to be an association between Env-specific B cells and the number of challenges required for SHIV infection. To adjust for multiple

comparisons, the BH procedure was used to control the FDR. An adjustment to control the FDR at an α value of 0.05 was performed for these prespecified correlation endpoints for a total 6 parameters (Table 2).

SUPPLEMENTAL MATERIAL

Supplemental material is available online only.

FIG S1, EPS file, 0.3 MB.

ACKNOWLEDGMENTS

The work was supported by National Institutes of Health grants 1R56 DE026321 (KDP), P01 AI117915 (S.R.P. and K.D.P.), T32 5108303 (A.D.C.), T32AI007392-31 (S.J.B.), the Office of Research Infrastructure Programs/OD P51OD011107 (to CNPRC), and the Center for AIDS Research award P30AI050410 (to UNC). The UNC Flow Cytometry Core Facility is supported in part by Cancer Center Core Support Grant P30 CA016086 to the UNC Lineberger Comprehensive Cancer Center. Research reported in this publication was supported by Center for AIDS Research award number 5P30AI050410.

The content is solely the responsibility of the authors and does not necessarily represent the official views of the National Institutes of Health.

We thank Sampa Santra (Harvard University) for kindly providing the SHIV-1157 (QNE)Y173H viral stock, Tomáš Hanke (Oxford University, Oxford, UK) for the ChAdOx1.tSIVconsV239 and MVA.tSIVconsV239 vaccines, and IDRI for 3M-052-SE.

We are grateful for technical assistance by the CNPRC staff, Jennifer Watanabe, Jodie Usachenko, Amir Ardeshir (CNPRC at UCD), Robert L. Wilson (LSUHSC), R. Whitney Edwards, Nicole Rodgers (Duke University), Neelima Choudary, and Ryan H. Tuck (UNC). We also acknowledge Celia LaBranche and colleagues (Duke University) for performing neutralization assays and David J. Pickup (Duke University) for development and production of the recombinant MVA-based vaccine.

We thank J. Lifson, Rebecca Shoemaker, and their colleagues in the Quantitative Molecular Diagnostics Core of the AIDS and Cancer Virus Program of the Frederick National Laboratory for expert assistance with viral load measurements.

REFERENCES

- UNAIDS. 2018. Global HIV & AIDS statistics—2018 fact sheet. <https://www.unaids.org>.
- Drake AL, Wagner A, Richardson B, John-Stewart G. 2014. Incident HIV during pregnancy and postpartum and risk of mother-to-child HIV transmission: a systematic review and meta-analysis. *PLoS Med* 11:e1001608. <https://doi.org/10.1371/journal.pmed.1001608>.
- Haas AD, Msukwa MT, Egger M, Tenthani L, Tweya H, Jahn A, Gadabu OJ, Tal K, Salazar-Vizcaya L, Estill J, Spoerri A, Phiri N, Chimbwandira F, van Oosterhout JJ, Keiser O. 2016. Adherence to antiretroviral therapy during and after pregnancy: cohort study on women receiving care in Malawi's Option B+ program. *Clin Infect Dis* 63:1227–1235. <https://doi.org/10.1093/cid/ciw500>.
- Myer L, Phillips TK, McIntyre JA, Hsiao NY, Petro G, Zerbe A, Ramjith J, Bekker LG, Abrams EJ. 2017. HIV viraemia and mother-to-child transmission risk after antiretroviral therapy initiation in pregnancy in Cape Town, South Africa. *HIV Med* 18:80–88. <https://doi.org/10.1111/hiv.12397>.
- Moland KM, de Paoli MM, Sellen DW, van Esterik P, Leshabari SC, Blystad A. 2010. Breastfeeding and HIV: experiences from a decade of prevention of postnatal HIV transmission in sub-Saharan Africa. *Int Breastfeed J* 5:10. <https://doi.org/10.1186/1746-4358-5-10>.
- Rollins N, Coovadia HM. 2013. Breastfeeding and HIV transmission in the developing world: past, present, future. *Curr Opin HIV AIDS* 8:467–473. <https://doi.org/10.1097/COH.0b013e3283632ba2>.
- Rollins NC, Ndirangu J, Bland RM, Coutousdis A, Coovadia HM, Newell ML. 2013. Exclusive breastfeeding, diarrhoeal morbidity and all-cause mortality in infants of HIV-infected and HIV uninfected mothers: an intervention cohort study in KwaZulu Natal, South Africa. *PLoS One* 8:e81307. <https://doi.org/10.1371/journal.pone.0081307>.
- Nduati R, John G, Mbori-Ngacha D, Richardson B, Overbaugh J, Mwachira A, Ndinya-Achola J, Bwayo J, Onyango FE, Hughes J, Kreiss J. 2000. Effect of breastfeeding and formula feeding on transmission of HIV-1: a randomized clinical trial. *JAMA* 283:1167–1174. <https://doi.org/10.1001/jama.283.9.1167>.
- WHO. 2014. Global update on the health sector response to HIV, 2014. WHO, Geneva, Switzerland.
- Coutsoudis A, Dabis F, Fawzi W, Gaillard P, Haverkamp G, Harris DR, Jackson JB, Leroy V, Meda N, Msellati P, Newell M-L, Nsuati R, Read JS, Wiktor S, Breastfeeding and HIV International Transmission Study Group. 2004. Late postnatal transmission of HIV-1 in breast-fed children: an individual patient data meta-analysis. *J Infect Dis* 189:2154–2166.
- Taha TE, Hoover DR, Kumwenda NI, Fiscus SA, Kafulafula G, Nkhoma C, Chen S, Piwowar E, Broadhead RL, Jackson JB, Miotti PG. 2007. Late postnatal transmission of HIV-1 and associated factors. *J Infect Dis* 196:10–14. <https://doi.org/10.1086/518511>.
- Leroy V, Karon JM, Alioum A, Ekpini ER, van de Perre P, Greenberg AE, Msellati P, Hudgens M, Dabis F, Wiktor SZ, West Africa PSG. 2003. Postnatal transmission of HIV-1 after a maternal short-course zidovudine peripartum regimen in West Africa. *AIDS* 17:1493–1501. <https://doi.org/10.1097/00002030-200307040-00010>.
- Bispo S, Chikungu L, Rollins N, Siegfried N, Newell ML. 2017. Postnatal HIV transmission in breastfed infants of HIV-infected women on ART: a systematic review and meta-analysis. *J Int AIDS Soc* 20:21251. <https://doi.org/10.7448/IAS.20.1.21251>.
- Cournil A, De Vincenzi I, Gaillard P, Cames C, Fao P, Luchters S, Rollins N, Newell ML, Bork K, Read JS, Kesho Bora Study Group. 2013. Relationship between mortality and feeding modality among children born to HIV-infected mothers in a research setting: the Kesho Bora study. *AIDS* 27:1621–1630. <https://doi.org/10.1097/QAD.0b013e32835d5226>.
- Kuhn L, Aldrovandi GM, Sinkala M, Kankasa C, Semrau K, Kasonde P, Mwiya M, Tsai WY, Thea DM, Zambia Exclusive Breastfeeding Study (ZEBs). 2009. Differential effects of early weaning for HIV-free survival of children born to

- HIV-infected mothers by severity of maternal disease. *PLoS One* 4:e6059. <https://doi.org/10.1371/journal.pone.0006059>.
16. Kuhn L, Aldrovandi GM, Sinkala M, Kankasa C, Semrau K, Mwiya M, Kasonde P, Scott N, Vwalika C, Walter J, Bulterys M, Tsai WY, Thea DM, Zambia Exclusive Breastfeeding Study. 2008. Effects of early, abrupt weaning on HIV-free survival of children in Zambia. *N Engl J Med* 359: 130–141. <https://doi.org/10.1056/NEJMoa073788>.
 17. Kuhn L, Stein Z, Susser M. 2004. Preventing mother-to-child HIV transmission in the new millennium: the challenge of breast feeding. *Paediatr Perinat Epidemiol* 18:10–16. <https://doi.org/10.1111/j.1365-3016.2003.00528.x>.
 18. World Health Organization. 2010. Guidelines on HIV and infant feeding 2010: principles and recommendations for infant feeding in the context of HIV and a summary of evidence. WHO, Geneva, Switzerland.
 19. Hessel AJ, Jaworski JP, Epton E, Matsuda K, Pandey S, Kahl C, Reed J, Sutton WF, Hammond KB, Cheever TA, Barnette PT, Legasse AW, Planer S, Stanton JJ, Pegu A, Chen X, Wang K, Siess D, Burke D, Park BS, Axthelm MK, Lewis A, Hirsch VM, Graham BS, Mascola JR, Sacha JB, Haigwood NL. 2016. Early short-term treatment with neutralizing human monoclonal antibodies halts SHIV infection in infant macaques. *Nat Med* 22:362–368. <https://doi.org/10.1038/nm.4063>.
 20. Hessel AJ, Malherbe DC, Haigwood NL. 2018. Passive and active antibody studies in primates to inform HIV vaccines. *Expert Rev Vaccines* 17: 127–144. <https://doi.org/10.1080/14760584.2018.1425619>.
 21. Hessel AJ, Shapiro MB, Powell R, Malherbe DC, McBurney SP, Pandey S, Cheever T, Sutton WF, Kahl C, Park B, Zolla-Pazner S, Haigwood NL. 2018. Reduced cell-associated DNA and improved viral control in macaques following passive transfer of a single anti-V2 monoclonal antibody and repeated SHIV challenges. *J Virol* 92:e02198-17. <https://doi.org/10.1128/JVI.02198-17>.
 22. McFarland EJ, Cunningham CK, Muresan P, Capparelli EV, Perkowski C, Morgan P, Smith B, Hazra R, Purdue L, Harding PA, Theron G, Mujuru H, Agwu A, Purswani M, Rathore MH, Flach B, Taylor A, Lin BC, McDermott AB, Mascola JR, Graham BS, International Maternal Pediatric Adolescent AIDS Clinical Trials Network (IMPAACT) P1112 Team. 2021. Safety, tolerability, and pharmacokinetics of a long-acting broadly neutralizing human immunodeficiency virus type 1 (HIV-1) monoclonal antibody VRC01LS in HIV-1-exposed newborn infants. *J Infect Dis* 224:1916–1924. <https://doi.org/10.1093/infdis/jiab229>.
 23. Corey L, Gilbert PB, Juraska M, Montefiori DC, Morris L, Karuna ST, Edupuganti S, Mgodini NM, deCamp AC, Rudnicki E, Huang Y, Gonzales P, Cabello R, Orrell C, Lama JR, Laher F, Lazarus EM, Sanchez J, Frank I, Hinojosa J, Sobieszczyk ME, Marshall KE, Mukwekwerere PG, Makhema J, Baden LR, Mullins JI, Williamson C, Hural J, McElrath MJ, Bentley C, Takuva S, Gomez Lorenzo MM, Burns DN, Espy N, Randhawa AK, Kochar N, Piwowar-Manning E, Donnell DJ, Sista N, Andrew P, Kublin JG, Gray G, Ledgerwood JE, Mascola JR, Cohen MS, HVTN 704/HPTN 085 and HVTN 703/HPTN 081 Study Teams. 2021. Two randomized trials of neutralizing antibodies to prevent HIV-1 acquisition. *N Engl J Med* 384:1003–1014. <https://doi.org/10.1056/NEJMoa2031738>.
 24. Mgodini NM, Takuva S, Edupuganti S, Karuna S, Andrew P, Lazarus E, Garnett P, Shava E, Mukwekwerere PG, Kochar N, Marshall K, Rudnicki E, Juraska M, Anderson M, Karg C, Tindale I, Greene E, Luthuli N, Baepanye K, Hural J, Gomez Lorenzo MM, Burns D, Miner MD, Ledgerwood J, Mascola JR, Donnell D, Cohen MS, Corey L, HVTN 703/HPTN 081 Team. 2021. A phase 2b study to evaluate the safety and efficacy of VRC01 broadly neutralizing monoclonal antibody in reducing acquisition of HIV-1 infection in women in Sub-Saharan Africa: baseline findings. *J Acquir Immune Defic Syndr* 87:680–687. <https://doi.org/10.1097/QAI.0000000000002649>.
 25. Ackerman ME, Das J, Pittala S, Broge T, Linde C, Suscovich TJ, Brown EP, Bradley T, Natarajan H, Lin S, Sassic JK, O'Keefe S, Mehta N, Goodman D, Sips M, Weiner JA, Tomaras GD, Haynes BF, Lauffenburger DA, Bailey-Kellogg C, Roederer M, Alter G. 2018. Route of immunization defines multiple mechanisms of vaccine-mediated protection against SIV. *Nat Med* 24:1590–1598. <https://doi.org/10.1038/s41591-018-0161-0>.
 26. Barouch DH, Alter G, Broge T, Linde C, Ackerman ME, Brown EP, Borducchi EN, Smith KM, Nkolola JP, Liu J, Shields J, Parenteau L, Whitney JB, Abbink P, Ng'ang'a DM, Seaman MS, Lavine CL, Perry JR, Li W, Colantonio AD, Lewis MG, Chen B, Wenschuh H, Reimer U, Piatak M, Lifson JD, Handley SA, Virgin HW, Koutsoukos M, Lorin C, Voss G, Weijtens M, Pau MG, Schuitemaker H. 2015. Protective efficacy of adenovirus/protein vaccines against SIV challenges in rhesus monkeys. *Science* 349: 320–324. <https://doi.org/10.1126/science.aab3886>.
 27. Barouch DH, Stephenson KE, Borducchi EN, Smith K, Stanley K, McNally AG, Liu J, Abbink P, Maxfield LF, Seaman MS, Dugast AS, Alter G, Ferguson M, Li W, Earl PL, Moss B, Giorgi EE, Szinger JJ, Eller LA, Billings EA, Rao M, Tovanabutra S, Sanders-Buell E, Weijtens M, Pau MG, Schuitemaker H, Robb ML, Kim JH, Korber BT, Michael NL. 2013. Protective efficacy of a rhesus HIV-1 mosaic vaccine against heterologous SHIV challenges in global monkeys. *Cell* 155:531–539. <https://doi.org/10.1016/j.cell.2013.09.061>.
 28. Bradley T, Pollara J, Santra S, Vandergrift N, Pittala S, Bailey-Kellogg C, Shen X, Parks R, Goodman D, Eaton A, Balachandran H, Mach LV, Saunders KO, Weiner JA, Searce R, Sutherland LL, Phogat S, Tartaglia J, Reed SG, Hu SL, Theis JF, Pinter A, Montefiori DC, Kepler TB, Peachman KK, Rao M, Michael NL, Suscovich TJ, Alter G, Ackerman ME, Moody MA, Liao HX, Tomaras G, Ferrari G, Korber BT, Haynes BF. 2017. Pentavalent HIV-1 vaccine protects against simian-human immunodeficiency virus challenge. *Nat Commun* 8:15711. <https://doi.org/10.1038/ncomms15711>.
 29. Fouts TR, Bagley K, Prado IJ, Bobb KL, Schwartz JA, Xu R, Zagursky RJ, Egan MA, Eldridge JH, LaBranche CC, Montefiori DC, Le Buanec H, Zagury D, Pal R, Pavlakis GN, Felber BK, Franchini G, Gordon S, Vaccari M, Lewis GK, DeVico AL, Gallo RC. 2015. Balance of cellular and humoral immunity determines the level of protection by HIV vaccines in rhesus macaque models of HIV infection. *Proc Natl Acad Sci U S A* 112:E992–E999. <https://doi.org/10.1073/pnas.1423669112>.
 30. Rerks-Ngarm S, Paris RM, Chunsutthiwat S, Prensri N, Namwat C, Bowonwatanuwong C, Li SS, Kaewkungkal J, Trichavaroj R, Churichanon N, de Souza MS, Andrews C, Francis D, Adams E, Flores J, Gurunathan S, Tartaglia J, O'Connell RJ, Eamsila C, Nitayaphan S, Nguay V, Thongcharoen P, Kunasol P, Michael NL, Robb ML, Gilbert PB, Kim JH. 2013. Extended evaluation of the virologic, immunologic, and clinical course of volunteers who acquired HIV-1 infection in a phase III vaccine trial of ALVAC-HIV and AIDSVAX B/E. *J Infect Dis* 207:1195–1205. <https://doi.org/10.1093/infdis/jis478>.
 31. Asokan M, Dias J, Liu C, Maximova A, Ernste K, Pegu A, McKeel K, Shi W, Chen X, Almasri C, Promsote W, Ambrozak DR, Gama L, Hu J, Douek DC, Todd JP, Lifson JD, Fourati S, Sekaly RP, Crowley AR, Ackerman ME, Ko SH, Kilam D, Boritz EA, Liao LE, Best K, Perelson AS, Mascola JR, Koup RA. 2020. Fc-mediated effector function contributes to the in vivo antiviral effect of an HIV neutralizing antibody. *Proc Natl Acad Sci U S A* 117: 18754–18763. <https://doi.org/10.1073/pnas.2008236117>.
 32. Wang P, Gajjar MR, Yu J, Padte NN, Gettie A, Blanchard JL, Russell-Lodrigue K, Liao LE, Perelson AS, Huang Y, Ho DD. 2020. Quantifying the contribution of Fc-mediated effector functions to the antiviral activity of anti-HIV-1 IgG1 antibodies in vivo. *Proc Natl Acad Sci U S A* 117: 18002–18009. <https://doi.org/10.1073/pnas.2008190117>.
 33. Phillips B, Fouda GG, Eudailey J, Pollara J, Curtis AD, Il, Kunz E, Dennis M, Shen X, Bay C, Hudgens M, Pickup D, Alam SM, Ardeshir A, Kozlowski PA, Van Rompay KKA, Ferrari G, Moody MA, Permar S, De Paris K. 2017. Impact of poxvirus vector priming, protein coadministration, and vaccine intervals on HIV gp120 vaccine-elicited antibody magnitude and function in infant macaques. *Clin Vaccine Immunol* 24:e00231-17. <https://doi.org/10.1128/CI.00231-17>.
 34. Phillips B, Van Rompay KKA, Rodriguez-Nieves J, Lorin C, Koutsoukos M, Tomai M, Fox CB, Eudailey J, Dennis M, Alam SM, Hudgens M, Fouda G, Pollara J, Moody A, Shen X, Ferrari G, Permar S, De Paris K. 2018. Adjuvant-dependent enhancement of HIV Env-specific antibody responses in infant rhesus macaques. *J Virol* 92:e01051-18. <https://doi.org/10.1128/JVI.01051-18>.
 35. Dennis M, Eudailey J, Pollara J, McMillan AS, Cronin KD, Saha PT, Curtis AD, Hudgens MG, Fouda GG, Ferrari G, Alam M, Van Rompay KKA, De Paris K, Permar S, Shen X. 2019. Coadministration of CH31 broadly neutralizing antibody does not affect development of vaccine-induced anti-HIV-1 envelope antibody responses in infant rhesus macaques. *J Virol* 93: e01783-18. <https://doi.org/10.1128/JVI.01783-18>.
 36. Kramski M, Schorcht A, Johnston AP, Lichtfuss GF, Jegaskanda S, De Rose R, Stratov I, Kelleher AD, French MA, Center RJ, Jaworowski A, Kent SJ. 2012. Role of monocytes in mediating HIV-specific antibody-dependent cellular cytotoxicity. *J Immunol Methods* 384:51–61. <https://doi.org/10.1016/j.jim.2012.07.006>.
 37. Pollara J, Orlandi C, Beck C, Edwards RW, Hu Y, Liu S, Wang S, Koup RA, Denny TN, Lu S, Tomaras GD, DeVico A, Lewis GK, Ferrari G. 2018. Application of area scaling analysis to identify natural killer cell and monocyte involvement in the GranToxiLux antibody dependent cell-mediated cytotoxicity assay. *Cytometry A* 93:436–447. <https://doi.org/10.1002/cyto.a.23348>.
 38. Hladik F, McElrath MJ. 2008. Setting the stage: host invasion by HIV. *Nat Rev Immunol* 8:447–457. <https://doi.org/10.1038/nri2302>.
 39. Chenine AL, Siddappa NB, Kramer VG, Sciaranghella G, Rasmussen RA, Lee SJ, Santosuosso M, Poznansky MC, Velu V, Amara RR, Souder C, Anderson DC, Villinger F, Else JG, Novembre FJ, Strobert E, O'Neil SP, Evan Secor W,

- Ruprecht RM. 2010. Relative transmissibility of an R5 clade C simian-human immunodeficiency virus across different mucosae in macaques parallels the relative risks of sexual HIV-1 transmission in humans via different routes. *J Infect Dis* 201:1155–1163. <https://doi.org/10.1086/651274>.
40. Jensen K, Dela Pena-Ponce MG, Piatak M, Jr, Shoemaker R, Oswald K, Jacobs WR, Jr, Fennelly G, Lucero C, Mollan KR, Hudgens MG, Amedee A, Kozlowski PA, Estes JD, Lifson JD, Van Rompay KK, Larsen M, De Paris K. 2017. Balancing trained immunity with persistent immune activation and the risk of SIV infection in infant macaques vaccinated with attenuated *Mycobacterium tuberculosis* or BCG vaccines. *Clin Vaccine Immunol* 24:e00360-16. <https://doi.org/10.1128/CI.00360-16>.
 41. Eudailey JA, Dennis ML, Parker ME, Phillips BL, Huffman TN, Bay CP, Hudgens MG, Wiseman RW, Pollara JJ, Fouda GG, Ferrari G, Pickup DJ, Kozlowski PA, Van Rompay KKA, De Paris K, Permar SR. 2018. Maternal HIV-1 Env vaccination for systemic and breast milk immunity to prevent oral SHIV acquisition in infant macaques. *mSphere* 3:e00505-17. <https://doi.org/10.1128/mSphere.00505-17>.
 42. Curtis AD, II, Dennis M, Eudailey J, Walter KL, Cronin K, Alam SM, Choudhary N, Tuck RH, Hudgens M, Kozlowski PA, Pollara J, Ferrari G, Van Rompay KKA, Permar S, De Paris K. 2020. HIV Env-specific IgG antibodies induced by vaccination of neonatal rhesus macaques persist and can be augmented by a late booster immunization in infancy. *mSphere* 5:e00162-20. <https://doi.org/10.1128/mSphere.00162-20>.
 43. Gomez-Roman VR, Patterson LJ, Venzon D, Liewehr D, Aldrich K, Florese R, Robert-Guroff M. 2005. Vaccine-elicited antibodies mediate antibody-dependent cellular cytotoxicity correlated with significantly reduced acute viremia in rhesus macaques challenged with SIVmac251. *J Immunol* 174:2185–2189. <https://doi.org/10.4049/jimmunol.174.4.2185>.
 44. Xiao P, Zhao J, Patterson LJ, Brocca-Cofano E, Venzon D, Kozlowski PA, Hidajat R, Demberg T, Robert-Guroff M. 2010. Multiple vaccine-elicited nonneutralizing anti-envelope antibody activities contribute to protective efficacy by reducing both acute and chronic viremia following simian/human immunodeficiency virus SHIV89.6P challenge in rhesus macaques. *J Virol* 84:7161–7173. <https://doi.org/10.1128/JVI.00410-10>.
 45. Alpert MD, Harvey JD, Lauer WA, Reeves RK, Piatak M, Jr, Carville A, Mansfield KG, Lifson JD, Li W, Desrosiers RC, Johnson RP, Evans DT. 2012. ADCC develops over time during persistent infection with live-attenuated SIV and is associated with complete protection against SIV(mac) 251 challenge. *PLoS Pathog* 8:e1002890. <https://doi.org/10.1371/journal.ppat.1002890>.
 46. Sheets RL, Zhou T, Knezevic I. 2016. Review of efficacy trials of HIV-1/AIDS vaccines and regulatory lessons learned: a review from a regulatory perspective. *Biologicals* 44:73–89. <https://doi.org/10.1016/j.biologicals.2015.10.004>.
 47. Qureshi H, Genesca M, Fritts L, McChesney MB, Robert-Guroff M, Miller CJ. 2014. Infection with host-range mutant adenovirus 5 suppresses innate immunity and induces systemic CD4+ T cell activation in rhesus macaques. *PLoS One* 9:e106004. <https://doi.org/10.1371/journal.pone.0106004>.
 48. Naranbhai V, Abdool Karim SS, Altfeld M, Samsunder N, Durgiah R, Sibeko S, Abdool Karim Q, Carr WH, CAPRISA004 TRAPS team. 2012. Innate immune activation enhances HIV acquisition in women, diminishing the effectiveness of tenofovir microbicide gel. *J Infect Dis* 206:993–1001. <https://doi.org/10.1093/infdis/jis465>.
 49. Huang Y, Duerr A, Frahm N, Zhang L, Moodie Z, De Rosa S, McElrath MJ, Gilbert PB. 2014. Immune-correlates analysis of an HIV-1 vaccine efficacy trial reveals an association of nonspecific interferon-gamma secretion with increased HIV-1 infection risk: a cohort-based modeling study. *PLoS One* 9:e108631. <https://doi.org/10.1371/journal.pone.0108631>.
 50. Hammer SM, Sobieszczyk ME, Janes H, Karuna ST, Mulligan MJ, Grove D, Koblin BA, Buchbinder SP, Keefer MC, Tomaras GD, Frahm N, Hural J, Anude C, Graham BS, Enama ME, Adams E, DeJesus E, Novak RM, Frank I, Bentley C, Ramirez S, Fu R, Koup RA, Mascola JR, Nabel GJ, Montefiori DC, Kublin J, McElrath MJ, Corey L, Gilbert PB, HVTN 505 Study Team. 2013. Efficacy trial of a DNA/rAd5 HIV-1 preventive vaccine. *N Engl J Med* 369:2083–2092. <https://doi.org/10.1056/NEJMoa1310566>.
 51. Pauthner MG, Nkolola JP, Havenar-Daughton C, Murrell B, Reiss SM, Bastidas R, Prevost J, Nedellec R, von Bredow B, Abbink P, Cottrell CA, Kulp DW, Tokatlian T, Nogal B, Bianchi M, Li H, Lee JH, Butera ST, Evans DT, Hangartner L, Finzi A, Wilson IA, Wyatt RT, Irvine DJ, Schief WR, Ward AB, Sanders RW, Crotty S, Shaw GM, Barouch DH, Burton DR. 2019. Vaccine-induced protection from homologous tier 2 SHIV challenge in non-human primates depends on serum-neutralizing antibody titers. *Immunity* 50:241–252.e6. <https://doi.org/10.1016/j.immuni.2018.11.011>.
 52. Florese RH, Van Rompay KK, Aldrich K, Forthall DN, Landucci G, Mahalanabis M, Haigwood N, Venzon D, Kalyanaraman VS, Marthas ML, Robert-Guroff M. 2006. Evaluation of passively transferred, nonneutralizing antibody-dependent cellular cytotoxicity-mediating IgG in protection of neonatal rhesus macaques against oral SIVmac251 challenge. *J Immunol* 177:4028–4036. <https://doi.org/10.4049/jimmunol.177.6.4028>.
 53. Dugast AS, Chan Y, Hoffner M, Licht A, Nkolola J, Li H, Streeck H, Suscovich TJ, Ghebremichael M, Ackerman ME, Barouch DH, Alter G. 2014. Lack of protection following passive transfer of polyclonal highly functional low-dose non-neutralizing antibodies. *PLoS One* 9:e97229. <https://doi.org/10.1371/journal.pone.0097229>.
 54. Haynes BF, Gilbert PB, McElrath MJ, Zolla-Pazner S, Tomaras GD, Alam SM, Evans DT, Montefiori DC, Karnasuta C, Sutthent R, Liao HX, DeVico AL, Lewis GK, Williams C, Pinter A, Fong Y, Janes H, DeCamp A, Huang Y, Rao M, Billings E, Karasavvas N, Robb ML, Ngauy V, de Souza MS, Paris R, Ferrari G, Bailer RT, Soderberg KA, Andrews C, Berman PW, Frahm N, De Rosa SC, Alpert MD, Yates NL, Shen X, Koup RA, Pitisuttithum P, Kaewkungwal J, Nitayaphan S, Rerks-Ngarm S, Michael NL, Kim JH. 2012. Immune-correlates analysis of an HIV-1 vaccine efficacy trial. *N Engl J Med* 366:1275–1286. <https://doi.org/10.1056/NEJMoa1113425>.
 55. Pollara J, Bonsignori M, Moody MA, Liu P, Alam SM, Hwang KK, Gurley TC, Kozink DM, Armand LC, Marshall DJ, Whitesides JF, Kaewkungwal J, Nitayaphan S, Pitisuttithum P, Rerks-Ngarm S, Robb ML, O'Connell RJ, Kim JH, Michael NL, Montefiori DC, Tomaras GD, Liao HX, Haynes BF, Ferrari G. 2014. HIV-1 vaccine-induced C1 and V2 Env-specific antibodies synergize for increased antiviral activities. *J Virol* 88:7715–7726. <https://doi.org/10.1128/JVI.00156-14>.
 56. Lewis GK, Finzi A, DeVico AL, Pazgier M. 2015. Conformational masking and receptor-dependent unmasking of highly conserved env epitopes recognized by non-neutralizing antibodies that mediate potent ADCC against HIV-1. *Viruses* 7:5115–5132. <https://doi.org/10.3390/v7092856>.
 57. Lu LL, Suscovich TJ, Fortune SM, Alter G. 2018. Beyond binding: antibody effector functions in infectious diseases. *Nat Rev Immunol* 18:46–61. <https://doi.org/10.1038/nri.2017.106>.
 58. Lewis GK. 2013. Qualitative and quantitative variables that affect the potency of Fc-mediated effector function in vitro and in vivo: considerations for passive immunization using non-neutralizing antibodies. *Curr HIV Res* 11:354–364. <https://doi.org/10.2174/1570162x113116660060>.
 59. Parker SJ, Sadlon TA, Gordon DL. 1995. Enhancement of NK cell-mediated antibody-dependent lysis of recombinant gp120-coated CD4 cells by complement. *J Infect Dis* 171:186–189. <https://doi.org/10.1093/infdis/171.1.186>.
 60. Tabora CP, Rivera J, Zaragoza O, Casadevall A. 2003. More is not necessarily better: prozone-like effects in passive immunization with IgG. *J Immunol* 170:3621–3630. <https://doi.org/10.4049/jimmunol.170.7.3621>.
 61. Li SS, Gilbert PB, Carpp LN, Pyo CW, Janes H, Fong Y, Shen X, Neidich SD, Goodman D, deCamp A, Cohen KW, Ferrari G, Hammer SM, Sobieszczyk ME, Mulligan MJ, Buchbinder SP, Keefer MC, DeJesus E, Novak RM, Frank I, McElrath MJ, Tomaras GD, Geraghty DE, Peng X. 2019. Fc gamma receptor polymorphisms modulated the vaccine effect on HIV-1 risk in the HVTN 505 HIV vaccine trial. *J Virol* 93:e2041-18. <https://doi.org/10.1128/JVI.02041-18>.
 62. Neidich SD, Fong Y, Li SS, Geraghty DE, Williamson BD, Young WC, Goodman D, Seaton KE, Shen X, Sawant S, Zhang L, deCamp AC, Blette BS, Shao M, Yates NL, Feely F, Pyo CW, Ferrari G, Team H, Frank I, Karuna ST, Swann EM, Mascola JR, Graham BS, Hammer SM, Sobieszczyk ME, Corey L, Janes HE, McElrath MJ, Gottardo R, Gilbert PB, Tomaras GD, HVTN 505 Team. 2019. Antibody Fc effector functions and IgG3 associate with decreased HIV-1 risk. *J Clin Invest* 129:4838–4849. <https://doi.org/10.1172/JCI126391>.
 63. Su B, Dispinseri S, Iannone V, Zhang T, Wu H, Carapito R, Bahram S, Scarlatti G, Moog C. 2019. Update on Fc-mediated antibody functions against HIV-1 beyond neutralization. *Front Immunol* 10:2968. <https://doi.org/10.3389/fimmu.2019.02968>.
 64. Pollara J, Tay MZ, Edwards RW, Goodman D, Crowley AR, Edwards RJ, Easterhoff D, Conley HE, Hoxie T, Gurley T, Jones C, Machiele E, Tuyishime M, Donahue E, Jha S, Spreng RL, Hope TJ, Wiehe K, He MM, Moody MA, Saunders KO, Ackerman ME, Ferrari G, Tomaras GD. 2021. Functional homology for antibody-dependent phagocytosis across humans and rhesus macaques. *Front Immunol* 12:678511. <https://doi.org/10.3389/fimmu.2021.678511>.
 65. Hallberg A, Malmstrom P. 1982. Natural killer cell activity and antibody-dependent cellular cytotoxicity in newborn infants. *Acta Paediatr Scand* 71:431–436. <https://doi.org/10.1111/j.1651-2227.1982.tb09447.x>.

66. PrabhuDas M, Adkins B, Gans H, King C, Levy O, Ramilo O, Siegrist CA. 2011. Challenges in infant immunity: implications for responses to infection and vaccines. *Nat Immunol* 12:189–194. <https://doi.org/10.1038/ni0311-189>.
67. Kollmann TR, Kampmann B, Mazmanian SK, Marchant A, Levy O. 2017. Protecting the newborn and young infant from infectious diseases: lessons from immune ontogeny. *Immunity* 46:350–363. <https://doi.org/10.1016/j.immuni.2017.03.009>.
68. Smolen KK, Ruck CE, Fortuno ES, Ho K, Dimitriu P, Mohn WW, Speert DP, Cooper PJ, Esser M, Goetghebuer T, Marchant A, Kollmann TR. 2014. Pattern recognition receptor-mediated cytokine response in infants across 4 continents. *J Allergy Clin Immunol* 133:818–826.e4. <https://doi.org/10.1016/j.jaci.2013.09.038>.
69. Corbett NP, Blimkie D, Ho KC, Cai B, Sutherland DP, Kallos A, Crabtree J, Rein-Weston A, Lavoie PM, Turvey SE, Hawkins NR, Self SG, Wilson CB, Hajjar AM, Fortuno ES, Kollmann TR. 2010. Ontogeny of Toll-like receptor mediated cytokine responses of human blood mononuclear cells. *PLoS One* 5:e15041. <https://doi.org/10.1371/journal.pone.0015041>.
70. Levy O. 2007. Innate immunity of the newborn: basic mechanisms and clinical correlates. *Nat Rev Immunol* 7:379–390. <https://doi.org/10.1038/nri2075>.
71. Kohl S, Loo LS, Gonik B. 1984. Analysis in human neonates of defective antibody-dependent cellular cytotoxicity and natural killer cytotoxicity to herpes simplex virus-infected cells. *J Infect Dis* 150:14–19. <https://doi.org/10.1093/infdis/150.1.14>.
72. Fairchild KD, Hudson RG, Douglas SD, McKenzie SE, Polin RA. 1996. Effect of gamma interferon on expression of Fc gamma receptors in monocytes of newborn infants and adults. *Clin Diagn Lab Immunol* 3:464–469. <https://doi.org/10.1128/cdli.3.4.464-469.1996>.
73. National Research Council. 2011. Guide for the care and use of laboratory animals, 8th ed. National Academies Press, Washington, DC.
74. Curtis AD, II, Walter KA, Nabi R, Jensen K, Dwivedi A, Pollara J, Ferrari G, Van Rompay KKA, Amara RR, Kozlowski PA, De Paris K. 2019. Oral coadministration of an intramuscular DNA/modified vaccinia Ankara vaccine for simian immunodeficiency virus is associated with better control of infection in orally exposed infant macaques. *AIDS Res Hum Retroviruses* 35:310–325. <https://doi.org/10.1089/AID.2018.0180>.
75. Moldt B, Le KM, Carnathan DG, Whitney JB, Schultz N, Lewis MG, Borducchi EN, Smith KM, Mackel JJ, Sweat SL, Hodges AP, Godzik A, Parren PW, Silvestri G, Barouch DH, Burton DR. 2016. Neutralizing antibody affords comparable protection against vaginal and rectal simian/human immunodeficiency virus challenge in macaques. *AIDS* 30:1543–1551. <https://doi.org/10.1097/QAD.0000000000001102>.
76. Van Rompay KKA, Curtis AD, Hudgens M, Tuck R, Choudhari N, Dennis M, Goswami R, Nelson A, Ruprecht RM, Shaw GM, Permar SR, De Paris K. 11 February 2019. Oral clade C SHIV challenge models to study pediatric HIV infection by breastmilk transmission. *bioRxiv* <https://doi.org/10.1101/545699>.
77. Jensen K, Nabi R, Van Rompay KK, Robichaux S, Lifson JD, Piatak M, Jr, Jacobs WR, Jr, Fennelly G, Canfield D, Mollan KR, Hudgens MG, Larsen MH, Amedee AM, Kozlowski PA, De Paris K. 2016. Vaccine-elicited mucosal and systemic antibody responses are associated with reduced simian immunodeficiency viremia in infant rhesus macaques. *J Virol* 90:7285–7302. <https://doi.org/10.1128/JVI.00481-16>.
78. Fouda GG, Eudailey J, Kunz EL, Amos JD, Liebl BE, Himes J, Boakye-Agyeman F, Beck K, Michaels AJ, Cohen-Wolkowicz M, Haynes BF, Reimann KA, Permar SR. 2017. Systemic administration of an HIV-1 broadly neutralizing dimeric IgA yields mucosal secretory IgA and virus neutralization. *Mucosal Immunol* 10:228–237. <https://doi.org/10.1038/mi.2016.32>.
79. Kozlowski PA, Lynch RM, Patterson RR, Cu-Uvin S, Flanigan TP, Neutra MR. 2000. Modified wick method using Weck-Cel sponges for collection of human rectal secretions and analysis of mucosal HIV antibody. *J Acquir Immune Defic Syndr* 24:297–309. <https://doi.org/10.1097/00126334-200008010-00001>.
80. Koene HR, Kleijer M, Algra J, Roos D, von Dem Borne AE, de Haas M. 1997. Fc gammaRIIIa-158V/F polymorphism influences the binding of IgG by natural killer cell Fc gammaRIIIa, independently of the Fc gammaRIIIa-48L/R/H phenotype. *Blood* 90:1109–1114. <https://doi.org/10.1182/blood.V90.3.1109>.
81. Garcia A, Keinonen S, Sanchez AM, Ferrari G, Denny TN, Moody MA. 2014. Leukopak PBMC sample processing for preparing quality control material to support proficiency testing programs. *J Immunol Methods* 409:99–106. <https://doi.org/10.1016/j.jim.2014.05.019>.
82. Sambor A, Garcia A, Berrong M, Pickeral J, Brown S, Rountree W, Sanchez A, Pollara J, Frahm N, Keinonen S, Kijak GH, Roederer M, Levine G, D'Souza MP, Jaimes M, Koup R, Denny T, Cox J, Ferrari G. 2014. Establishment and maintenance of a PBMC repository for functional cellular studies in support of clinical vaccine trials. *J Immunol Methods* 409:107–116. <https://doi.org/10.1016/j.jim.2014.04.005>.
83. Pollara J, Jones DJ, Huffman T, Edwards RW, Dennis M, Li SH, Jha S, Goodman D, Kumar A, LaBranche CC, Montefiori DC, Fouda GG, Hope TJ, Tomaras GD, Staats HF, Ferrari G, Permar SR. 2019. Bridging vaccine-induced HIV-1 neutralizing and effector antibody responses in rabbit and rhesus macaque animal models. *J Virol* 93:e02119-18. <https://doi.org/10.1128/JVI.02119-18>.
84. Edmonds TG, Ding H, Yuan X, Wei Q, Smith KS, Conway JA, Wiczorek L, Brown B, Polonis V, West JT, Montefiori DC, Kappes JC, Ochsenbauer C. 2010. Replication competent molecular clones of HIV-1 expressing Renilla luciferase facilitate the analysis of antibody inhibition in PBMC. *Virology* 408:1–13. <https://doi.org/10.1016/j.virol.2010.08.028>.
85. Tay MZ, Liu P, Williams LD, McRaven MD, Sawant S, Gurley TC, Xu TT, Dennison SM, Liao HX, Chenine AL, Alam SM, Moody MA, Hope TJ, Haynes BF, Tomaras GD. 2016. Antibody-mediated internalization of infectious HIV-1 virions differs among antibody isotypes and subclasses. *PLoS Pathog* 12:e1005817. <https://doi.org/10.1371/journal.ppat.1005817>.
86. Ackerman ME, Moldt B, Wyatt RT, Dugast AS, McAndrew E, Tsoukas S, Jost S, Berger CT, Sciaranghella G, Liu Q, Irvine DJ, Burton DR, Alter G. 2011. A robust, high-throughput assay to determine the phagocytic activity of clinical antibody samples. *J Immunol Methods* 366:8–19. <https://doi.org/10.1016/j.jim.2010.12.016>.
87. Pardi N, LaBranche CC, Ferrari G, Cain DW, Tombacz I, Parks RJ, Muramatsu H, Mui BL, Tam YK, Kariko K, Polacino P, Barbosa CJ, Madden TD, Hope MJ, Haynes BF, Montefiori DC, Hu SL, Weissman D. 2019. Characterization of HIV-1 nucleoside-modified mRNA vaccines in rabbits and rhesus macaques. *Mol Ther Nucleic Acids* 15:36–47. <https://doi.org/10.1016/j.omtn.2019.03.003>.
88. Montefiori DC. 2009. Measuring HIV neutralization in a luciferase reporter gene assay. *Methods Mol Biol* 485:395–405. https://doi.org/10.1007/978-1-59745-170-3_26.
89. Jensen K, Pena MG, Wilson RL, Ranganathan UD, Jacobs WR, Jr, Fennelly G, Larsen M, Van Rompay KK, Kozlowski PA, Abel K. 2013. A neonatal oral Mycobacterium tuberculosis-SIV prime/intramuscular MVA-SIV boost combination vaccine induces both SIV and Mtb-specific immune responses in infant macaques. *Trials Vaccinol* 2:53–63. <https://doi.org/10.1016/j.trivac.2013.09.005>.